

Randomized Time Riemannian Manifold Hamiltonian Monte Carlo

Peter A. Whalley*, Daniel Paulin* and Benedict Leimkuhler*

June 10, 2022

Abstract

In the last decade several sampling methods have been proposed which rely on piecewise deterministic Markov processes (PDMPs). PDMPs are based on following deterministic trajectories with stochastic events which correspond to jumps in the state space. We propose implementing constraints in this setting to exploit geometries of high-dimensional problems by introducing a PDMP version of Riemannian manifold Hamiltonian Monte Carlo, which we call randomized time Riemannian manifold Hamiltonian Monte Carlo. Efficient sampling on constrained spaces is also needed in many applications including protein conformation modelling, directional statistics and free energy computations. We will show how randomizing the duration parameter for Hamiltonian flow can improve the robustness of Riemannian manifold Hamiltonian Monte Carlo methods. We will then compare methods on some example distributions which arise in application and provide an application of sampling on manifolds in high-dimensional covariance estimation.

1 Introduction and Motivation

Efficient sampling of high dimensional probability distributions is required for Bayesian inference and is a challenge in many fields including biological modelling (Wilkinson (2007)), economic modelling (Greenberg (2012)), machine learning with large data sets (Pakman et al. (2017), Barber (2012)) and molecular dynamics (Perez et al. (2015)). A popular approach is Markov chain Monte Carlo, which defines a Markov chain $X_{i+1} \sim p(\cdot | X_i)$ with invariant measure μ and from which we may estimate expected values from the following relation:

$$\mathbb{E}_{X \sim \mu} f(X) \approx \frac{1}{N} \sum_{i=1}^N f(X_i).$$

A fundamental problem is that convergence of standard Monte Carlo methods can often become slow in high dimensions and for multimodal distributions (for example see Quiroz et al. (2018)). In the last decade several sampling methods for Bayesian inference have been proposed, for example the local bouncy particle sampler proposed in Bouchard-Côté et al. (2018) and the Zig-Zag process proposed in Bierkens et al. (2019). These methods

*Department of Mathematics, University of Edinburgh.

are based on a new framework which constructs a piecewise deterministic Markov process (PDMP) whose invariant distribution is the distribution of interest (see Vanetti et al. (2018)). Another PDMP considered by Bou-Rabee and Sanz-Serna (2017) and studied in Deligiannidis et al. (2021), is a variant of Hamiltonian Monte Carlo (HMC) in which Hamiltonian trajectories are evolved for a duration drawn from an exponential distribution; this is known as Randomized Hamiltonian Monte Carlo (RHMC). In standard HMC the choice of integration time is a challenging task (see Hoffman et al. (2014)); in particular it is possible to introduce inefficient mixing for certain choices of the integration time. By contrast, RHMC does not suffer from this problem as randomly drawing the integration time, according to an exponential distribution, prevents periodicities and provides a more robust method with respect to the choice of integration parameters. This strategy has been shown to fix the inefficient mixing problem analytically within the Gaussian framework, as well as numerically for a number of examples in Bou-Rabee and Sanz-Serna (2017). Several algorithms have been proposed recently which rely on this idea (for example Riou-Durand and Vogrinc (2022) and Kleppe (2022)).

All algorithms discussed so far are targeted to sampling from distributions in Euclidean space. For sampling on Riemannian manifolds and non-Euclidean spaces more care is needed to generate sample points which satisfy the constraints imposed by the manifold's structure. The need to work with Riemannian manifolds is motivated by applications where constraints are imposed from modelling considerations or introduced in order to restrict sampling to a relevant subdomain derived from statistical analysis (see Brubaker et al. (2012)). Typical manifolds include products of spheres or orthogonal matrices which arise in applications in protein configuration modelling with the Fisher-Bingham distribution (Hamelryck et al. (2006)), texture analysis using distributions over rotations (Kunze and Schaben (2004)) and fixed-rank matrix factorization for collaborative filtering (Meyer et al. (2011), Salakhutdinov and Mnih (2008)). Methods that sample from probability distributions on manifolds have been considered in Hartmann (2008), Brubaker et al. (2012), Byrne and Girolami (2013), Girolami and Calderhead (2011), Lelièvre et al. (2012), Zappa et al. (2018), Diaconis et al. (2013), Lelièvre et al. (2019) and Laurent and Vilmart (2021). In this article, we focus on manifolds which are defined by constraints (for example spheres, the torus, orthogonal groups). In order to maintain the constraints, in practice one needs to perform projections at each step of the algorithm, an additional overhead compared to Euclidean MCMC algorithms.

In this work we propose a constrained version of RHMC (Randomized Hamiltonian Monte Carlo). We refer to our algorithm as the Randomized Time Riemannian Manifold Hamiltonian Monte Carlo (RT-RMHMC) method. We establish invariance under a compactness assumption of the desired measure in the (small step size limit) continuous time PDMP version of our method, where the algorithm is rejection free. Further, we demonstrate the invariance of the discretized method with Metropolis-Hastings adjustment and provide an ergodicity result. We show in numerical experiments that this method has improved robustness, demonstrating for example that the convergence rate is relatively flat in the choice of mean time parameter; these results mirror those obtained for the Euclidean version of the method.

We also compare RT-RMHMC to a constrained underdamped Langevin integrator g-BAOAB introduced in Leimkuhler and Matthews (2016). g-BAOAB is a biased sampling method, but highly efficient. The bias creates errors in computed observables and the

method is most accurate in the highly damped regime, but in this limit convergence is slowed. This is particularly the case in metastable systems (multimodal distributions), where significant bias may be observed. Kleppe (2022) recently introduced a biased RHMC method which has event rates which depend on the position in the state space, these state dependent event rates can be incorporated into our RHMC Riemannian framework when the framework is unadjusted. We note that in the appendix of Kleppe (2022) they introduce a version of RHMC with an adapted metric, however in the setting of adapting the metric for sampling on Euclidean space rather than on a Riemannian manifold. There is no theoretical or numerical treatment of RHMC in the manifold setting. We focus here on Metropolis-Hastings-adjusted algorithms to exactly sample from the invariant measure, where we don't have to take bias into consideration.

2 Algorithm

Let (\mathcal{M}, g) be a d -dimensional Riemannian manifold and $T\mathcal{M}$ denote its tangent bundle. Let $G(x)$ denote the positive definite matrix associated to the metric g at $x \in \mathcal{M}$. Consider a target distribution on \mathcal{M} with density

$$\pi(x) = \frac{1}{Z_{\mathcal{M}}} \exp(-U(x)),$$

with respect to $\sigma_{\mathcal{M}}(dx)$, the surface measure of \mathcal{M} defined by $\sigma_{\mathcal{M}}(dx) = \sqrt{\det G(x)}dx$ and

$$Z_{\mathcal{M}} = \int_{\mathcal{M}} \exp(-U(x))\sigma_{\mathcal{M}}(dx),$$

which we assume to be finite.

Consider an extension of the distribution to $T\mathcal{M}$ as

$$\mu(dz) = \frac{1}{Z_{T\mathcal{M}}} \exp(-H(x, v))\lambda_{T\mathcal{M}}(dz), \quad (1)$$

where $\lambda_{T\mathcal{M}}(dz)$ is the Liouville measure of $T\mathcal{M}$, H is defined by

$$H(x, v) = U(x) + v^T G(x)^{-1}v \quad (2)$$

for $(x, v) \in T\mathcal{M}$ and

$$Z_{T\mathcal{M}} = \int_{T\mathcal{M}} \exp(-H(x, v))\lambda_{T\mathcal{M}}(dz),$$

which is finite when $Z_{\mathcal{M}}$ is.

Note that the Liouville measure has the following tensorization property (Lelièvre et al. (2010)[Proposition 3.40])

$$\lambda_{T\mathcal{M}}(dx dv) = \sigma_{\mathcal{M}}(dx)\sigma_{T_x\mathcal{M}}(dv),$$

where $\sigma_{T_x\mathcal{M}}(dv)$ is simply the Lebesgue measure on $T_x\mathcal{M}$. Due to this tensorization property we have that

$$\mu(dz) = \pi(x)\sigma_{\mathcal{M}}(dx)\psi(x)(dv),$$

where $\psi(x)(dv)$ is simply the Gaussian measure on $T_x\mathcal{M}$ given by

$$\psi(x)(dv) = \frac{1}{\sqrt{\{(2\pi)^d \det G(x)\}}} \exp\left\{-\frac{1}{2}v^T G(x)^{-1}v\right\} \sigma_{T_x\mathcal{M}}(dv)$$

in local coordinates and $\sigma_{T_x\mathcal{M}}(dv)$ is the Lebesgue measure on $T_x\mathcal{M}$. In particular we have that μ has marginal distribution π (Lelièvre et al. (2010)[Section 3.3.2]).

We will define a stochastic process which is a Riemannian version of the Randomized Hamiltonian Monte Carlo of Bou-Rabee and Sanz-Serna (2017). The stochastic process follows constrained Hamiltonian dynamics for an time duration t sampled from $t \sim \exp 1/\lambda$ for some rate $\lambda > 0$ before an event. This event is a random velocity refreshment under the distribution $\psi(x)$.

Algorithm 1 defines Randomized time Riemannian Manifold Hamiltonian Monte Carlo (RT-RMHMC) with rate parameter $\lambda > 0$, and Hamiltonian dynamics governed by the Hamiltonian $H(x, v) = U(x) + v^T G(x)^{-1}v$ defined on $T\mathcal{M}$. This stochastic process has invariant measure $\mu(z) = \exp(-H(z))$ with respect to the Liouville (surface) measure on $T\mathcal{M}$.

Algorithm 1: RT-RMHMC

- Initialise x_0 arbitrarily on \mathcal{M} and sample $v_0 \sim \psi(x_0)$ on $T_{x_0}\mathcal{M}$ such that $(x_0, v_0) \in T\mathcal{M}$.
 - Initialise $t_0 = 0$.
 - for $k = 1, 2, \dots$ do
 - Update time via $t_k = t_{k-1} + \delta t$, where $\delta t \sim \exp(1/\lambda)$.
 - Evolve over $[t_{k-1}, t_k]$ Hamilton's equations with initial condition $(x(t_{k-1}), v(t_{k-1})) = (x_{t_{k-1}}, v_{t_{k-1}})$.
 - Set
$$(x_s, v_s) = (x(s), v(s)) \text{ for } s \in [t_{k-1}, t_k].$$
 - Set $x_{t_k} = x(t_k)$.
 - Sample $v_{t_k} \sim \psi(x_{t_k})$ such that $(x_{t_k}, v_{t_k}) \in T\mathcal{M}$.
-

To sample from a distribution π with respect to the Hausdorff measure we define $U = -\log \pi$ under the assumption that π is integrable on \mathcal{M} .

We can define the generator for this stochastic process as

$$\mathcal{L}f(z) = X_H(f(z)) + \lambda_{ref}(Qf(z) - f(z)), \tag{3}$$

where

$$Qf(x, v) := \frac{1}{\sqrt{\{(2\pi)^d \det G(x)\}}} \int_{T_x\mathcal{M}} \exp\left\{-\frac{1}{2}\xi^T G(x)^{-1}\xi\right\} f(x, \xi) d\xi$$

is the transition kernel for a completely randomized velocity refreshment according to a Gaussian distribution on the tangent space $T_x\mathcal{M}$ and X_H is the Hamiltonian vector field associated to H . We will prove that this is the generator of this stochastic process in section 3 and invariance of the measure in section 4 under a compactness assumption.

3 Generator of RT-RMHMC

To prove that the generator of this stochastic process takes the form of equation 3 and that the measure (equation 1) is invariant under RT-RMHMC we use the framework of Durmus

et al. (2021) viewing RT-RMHMC as a piecewise deterministic Markov process (PDMP) defined on $T\mathcal{M}$. A \mathcal{Z} -valued continuous time PDMP (φ, λ, Q) consists of the following components:

- a differential flow φ on \mathcal{Z} which satisfies the semi group property and is measurable. Moreover, is continuously differentiable with respect to time and a C^1 -diffeomorphism of \mathcal{Z} .
- an event rate $\lambda : \mathcal{Z} \rightarrow \mathbb{R}^+$, which is measurable and locally bounded.
- a inhomogeneous Markov transition kernel $Q : \mathbb{R}_+ \times \mathcal{Z} \times \mathcal{B}(\mathcal{Z}) \rightarrow [0, 1]$, such that for all $A \in \mathcal{B}(\mathcal{Z})$, $(t, z) \mapsto Q(t, z, A)$ is measurable and for all $(t, z) \in \mathbb{R}_+ \times T\mathcal{M}$, $Q(t, z, \cdot) \in \mathcal{P}(\mathcal{Z})$,

where $\mathcal{B}(\mathcal{Z})$ denotes the σ -algebra on the space \mathcal{Z} and $\mathcal{P}(\mathcal{Z})$ denotes the space of probability measures on the space \mathcal{Z} . For RT-RMHMC we consider $\mathcal{Z} = T\mathcal{M}$.

Def 3.1. For a PDMP $Z = (Z_t)_{t \geq 0}$, we call $\tau_\infty(Z) = \inf\{t \geq 0 \mid Z_t = \infty\}$ the explosion time of the process $(Z_t)_{t \geq 0}$. A process $(Z_t)_{t \geq 0}$ is said to be non-explosive if $\tau_\infty(Z) = +\infty$ almost surely. PDMP characteristics are said to be non-explosive if for all initial distribution the associated PDMP is non-explosive.

Due to the event rate λ_{ref} of RT-RMHMC being constant and bounded we have that RT-RMHMC is non-explosive. As RT-RMHMC is a non-explosive PDMP we can use the theory of Durmus et al. (2021)[Section 7 and 8] to establish the generator and invariance of the desired measure.

Under the assumption that the expected number of events in any unit time interval $[0, t]$ is finite, it is shown in Davis (1993)[Theorem 26.14] that for a non-explosive PDMP with generator \mathcal{A} with domain $D(\mathcal{A})$ that all $f \in D(\mathcal{A})$ and $x \in T\mathcal{M}$,

$$\mathcal{A}f(x) = D_\varphi f(x) + \lambda(x)(Qf(x) - f(x)).$$

If we let N_t denote the number of events in the interval $[0, t]$ then we have for RT-RMHMC $\mathbb{E}_x(N_t) = \lambda_{ref}t < \infty$, \mathbb{E}_x denoting the expected value given the stochastic process starts with initial condition x . Therefore all the assumptions are satisfied of Davis (1993)[Theorem 26.14] and Durmus et al. (2021)[Section 7] and we have that the generator of RT-RMHMC is given by

$$\mathcal{L}f(x) = X_H(f) + \lambda_{ref}(Qf(x) - f(x)),$$

where X_H is the Hamiltonian vector field and Q is the transition kernel for the Gaussian distribution induced by the metric $G(x)$ on the tangent space of $x \in \mathcal{M}$.

4 Invariant measure

To prove that μ is an invariant measure of RT-RMHMC it is sufficient to show that $\int \mathcal{L}f(x)d\mu = 0$ for all $f \in D(\mathcal{L})$. As it is difficult to consider $D(\mathcal{L})$, one approach is to show that $C_c^1(T\mathcal{M})$ is a core of the generator and that $\int \mathcal{L}f(x)d\mu = 0$ for all $f \in C_c^1(T\mathcal{M})$, where $C_c^k(T\mathcal{M})$ denotes the space of k times differentiable functions $f : T\mathcal{M} \rightarrow \mathbb{R}$ with compact support.

Theorem 4.1 (Infinitesimal Invariance of RT-RMHMC). *Let \mathcal{M} be a smooth Riemannian manifold with metric g and let $(P_t)_{t \geq 0}$ be the semigroup of RT-RMHMC defined on \mathcal{M} with potential $U \in C^2(\mathcal{M})$ and Hamiltonian $H = U + K \in C^2(T\mathcal{M})$. Let μ be the measure on $(T\mathcal{M}, \mathcal{B}(T\mathcal{M}))$ defined by*

$$\mu(dz) \propto e^{-H(x,v)} d\lambda_{T\mathcal{M}}(z),$$

where $d\lambda_{T\mathcal{M}}$ is the Liouville measure of $T\mathcal{M}$. Then for all $f \in C_c^1(T\mathcal{M})$

$$\int_{T\mathcal{M}} \mathcal{L}f(x,v)\mu(dz) = 0,$$

where \mathcal{L} is the generator of RT-RMHMC.

Proof. We have that

$$\int_{T\mathcal{M}} \mathcal{L}f(x,v)\mu(dz) = \int_{T\mathcal{M}} X_H(f)d\mu + \lambda_{ref} \int_{T\mathcal{M}} (Q - I)f d\mu.$$

We will now consider these two integrals separately. Considering the first integral, due to the fact that μ is a Liouville measure, μ is invariant under the Hamiltonian flow by Liouville's theorem and hence the first integral is identically zero. Now considering the second integral we have

$$\begin{aligned} \int [Qf(x,v) - f(x,v)]\mu(dz) &= \int \int C(x) e^{-\frac{1}{2}\xi^T G(x)^{-1}\xi} (f(x,\xi) - f(x,v)) d\xi e^{-H(x,v)} d\lambda_{T\mathcal{M}}(z) \\ &= \int \int C(x) e^{-\frac{1}{2}\xi^T G(x)^{-1}\xi} e^{-U(x) - \frac{1}{2}v^T G(x)^{-1}v} (f(x,\xi) - f(x,v)) d\xi d\lambda_{T\mathcal{M}}(z) \\ &= \int C(x) e^{-U(x)} \int \int e^{-\frac{1}{2}\xi^T G(x)^{-1}\xi} e^{-\frac{1}{2}v^T G(x)^{-1}v} (f(x,\xi) - f(x,v)) d\xi dv d\sigma_{\mathcal{M}}(x) \\ &= 0, \end{aligned}$$

where $C(x)$ is a varying constant depending on x . Therefore we have that

$$\int_{T\mathcal{M}} \mathcal{L}f(x,v)\mu(dz) = 0,$$

and μ is an infinitesimally invariant measure. □

We will next demonstrate that $C_c^1(T\mathcal{M})$ is a core of $D(A)$ by showing that certain conditions established in Durmus et al. (2021) hold under the assumption that \mathcal{M} is compact. To show that $C_c^1(T\mathcal{M})$ is a core of $D(A)$ we use the approach of compactly approximating RT-RMHMC by a more well-behaved PDMP, which has PDMP characteristics $(\varphi, \lambda_{ref}, Q^\epsilon)$ satisfying the Assumption A3 from Durmus et al. (2021) and has a Feller transition semigroup $(P_t)_{t \geq 0}$. We then use this approximation to show that RT-RMHMC is Feller and $C_c^1(T\mathcal{M})$ is a core of the strong generator of RT-RMHMC, whose transition semigroup $(P_t)_{t \geq 0}$ is seen as a semigroup on $C_0(T\mathcal{M})$. Note that $C_0(T\mathcal{M})$ denotes the space of continuous functions $f : T\mathcal{M} \rightarrow \mathbb{R}$ that vanish at infinity and $C_0(T\mathcal{M})$ is a Banach space when equipped with the $\|\cdot\|_\infty$ norm.

We first approximate our PDMP (φ, λ, Q) (RT-RMHMC) with the PDMP with characteristics $(\varphi, \lambda_{ref}, Q^\epsilon)$ in the sense that

$$\sup_{z \in T\mathcal{M}, A \in \mathcal{B}(T\mathcal{M})} \{\lambda^\epsilon(z) \wedge \lambda(z) |Q^\epsilon(z, A) - Q(z, A)| + |\lambda^\epsilon(z) - \lambda(z)|\} \leq \epsilon,$$

where Q^ϵ is constructed as a Markov kernel corresponding to a consistently truncated Gaussian distribution on each tangent space as follows.

Define $G : \mathcal{M} \times \mathbb{R} \rightarrow \mathbb{R}$ by

$$G(x, a) = \int_{B(0, a)} \psi(x)(dv) - (1 - \epsilon/2\lambda_{ref}),$$

where $\psi(x)$ denotes the probability density function of the Gaussian distribution on $T_x\mathcal{M}$ defined by $\psi(x)(dv) = \exp(-\frac{1}{2}v^T G(x)^{-1}v)dv$, known as the Maxwellian distribution. Then we have that $\partial G/\partial a \neq 0$ due to the fact that $G(x, \cdot)$ is strictly increasing. By the implicit function theorem there exists a unique continuously differentiable function $M : \mathcal{M} \rightarrow \mathbb{R}$ such that $G(x, M(x)) = 0$ for all $x \in \mathcal{M}$. We define the transition kernel as follows:

$$Q^\epsilon(z, dz') = \lambda_{ref} \delta_x(dx') \psi_\epsilon(x)(dv'),$$

where

$$\psi_\epsilon(x)(dv') = \begin{cases} \frac{1}{1 - \epsilon/2\lambda_{ref}} \psi(x)(dv') & \text{for } |v'|_g \leq M(x) \\ 0 & \text{otherwise} \end{cases}$$

is the truncated Maxwellian distribution. Then we have that for any $(x, v) \in T\mathcal{M}$ and $A \in \mathcal{B}(T\mathcal{M})$

$$\begin{aligned} & |Q^\epsilon((x, v), A) - Q((x, v), A)| = \\ & = \lambda_{ref} \left| \left(\frac{1}{1 - \epsilon/2\lambda_{ref}} - 1 \right) \int_{A \cap B(0, M(x))} \psi(x)(dv') - \int_{A \cap B(0, M(x))^c} \psi(x)(dv') \right| \\ & \leq \lambda_{ref} \left(\frac{1}{1 - \epsilon/2\lambda_{ref}} - 1 \right) \left| \int_{A \cap B(0, M(x))} \psi(x)(dv') \right| + \lambda_{ref} \left| \int_{A \cap B(0, M(x))^c} \psi(x)(dv') \right| \\ & \leq \lambda_{ref} \left(\frac{1}{1 - \epsilon/2\lambda_{ref}} - 1 \right) (1 - \epsilon/2\lambda_{ref}) + \lambda_{ref} (1 - (1 - \epsilon/2\lambda_{ref})) \\ & = \epsilon. \end{aligned}$$

Lemma 4.2 (Continuity of Semigroup). *Let (\mathcal{M}, g) be a smooth Riemannian manifold, and let $U \in C^1(\mathcal{M})$ and hence $H \in C^1(T\mathcal{M})$. Let $(P_t)_{t \geq 0}$ be the transition semigroup of $(\varphi, \lambda_{ref}, Q^\epsilon)$, then*

$$|P_t f - f| \rightarrow 0 \text{ as } t \rightarrow 0, \text{ for all } f \in C_0(T\mathcal{M}).$$

Proof. Let $(Z_t)_{t \geq 0}$ denote a sample path of $(\varphi, \lambda_{ref}, Q^\epsilon)$. We have that

$$\begin{aligned} |P_t f(z) - f(z)| &= |\mathbb{E}_z(f(Z_t) - f(z))| \\ &= |\mathbb{E}_z(f(Z_t) \mathbb{1}(S_1 \leq t) + f(Z_t) \mathbb{1}(S_1 > t)) - f(z)| \\ &\leq \|f\|_\infty \mathbb{P}(S_1 \leq t) + |f(\varphi_t(z)) e^{-\lambda_{ref} t} - f(z)| \\ &= \|f\|_\infty (1 - e^{-\lambda_{ref} t}) + |f(\varphi_t(z)) - f(z)| \rightarrow 0, \end{aligned}$$

where S_1 is the time of the first event and $\varphi_t(z)$ is the solution of the Hamiltonian flow. If H is continuously differentiable everywhere then $\varphi_t(z)$ is well defined for all $t > 0$, and $\varphi_t(z) \rightarrow z$ as $t \rightarrow 0$ (see for example Chicone (2006)[Theorem 1.186]). \square

Lemma 4.3. *Let (\mathcal{M}, g) be a compact Riemannian manifold, and let $U \in C^1(\mathcal{M})$. Let $(\varphi, \lambda_{ref}, Q^\epsilon)$ be the PDMP approximation of RT-RMHMC defined above. The set of all possible sample paths of $(\varphi, \lambda_{ref}, Q^\epsilon)$ with initial condition (X_0, V_0) is contained in a compact set.*

Proof. Let $M(x)$ denote the continuous function in the definition of Q_ϵ which controls the truncation of the Gaussian distribution. $M(x)$ is a continuous function on a compact set and hence bounded by M_ϵ . We further choose M_ϵ such that $|V_0|_g \leq M_\epsilon$. Define the set

$$U_\epsilon = \{(x, v) \mid x \in \mathcal{M}, |v|_g \leq M_\epsilon\} \subset T\mathcal{M}.$$

Due to the fact that \mathcal{M} is compact it follows that U_ϵ is a compact subset of $T\mathcal{M}$ by Lemma A.1. We have that H restricted to U_ϵ is bounded by M_H as it's continuous on a compact set. We also have that H is constant between event times of the PDMP, by the definition of Hamiltonian flow. Therefore the Hamiltonian defined on the PDMP (X_t, V_t) takes values which are defined by the image of (X_{t_i}, V_{t_i}) , for events t_i $i = 1, 2, \dots$. At event time $t_i \sim \exp \lambda$, we have that $(X_{t_i}, V_{t_i}) \in U_\epsilon$, where $(X_{t_i}, V_{t_i}) \sim Q(X_{t_i-}, V_{t_i-}, \cdot)$. Therefore we can bound the Hamiltonian by M_H on $\{(X_t, V_t) \mid t \geq 0\}$. Now we have that

$$\begin{aligned} M_H &\geq H(X_t, V_t) = U(X_t) + |V_t|_g \\ &\geq m_U + |V_t|_g \end{aligned}$$

for all t . Therefore

$$\{(X_t, V_t) \mid t \geq 0\} \subset \{(x, v) \mid x \in \mathcal{M}, |v|_g \leq M_V := M_H - m_U\},$$

which is compact by Lemma A.1. \square

We have the following assumption from Durmus et al. (2021), which we use to establish Proposition 4.1.

Def 4.4. *Durmus et al. (2021)[Definition 16] We say that a homogeneous differential flow φ on $T\mathcal{M}$ and a homogeneous Markov kernel Q on $T\mathcal{M}$ are compactly compatible if for all compact sets $K \subset T\mathcal{M}$ and $T \geq 0$, there exists a compact set $\tilde{K} \subset T\mathcal{M}$ satisfying: for all $n \in \mathbb{N}^*$, $(t_i)_{i \in [1, n]} \in \mathbb{R}_+^n$, $\sum_{i=1}^n t_i \leq T$, there exists a sequence $(K_i)_{i \in [1, n]}$ of compact sets of $T\mathcal{M}$ such that, setting $K_0 = K$,*

1. for all $i \in [1, n]$, K_i only depends on $(t_j)_{j \in [1, n]}$ and $\cup_{i=0}^n K_i \subset \tilde{K}$;
2. for all $i \in [0, n-1]$, $s_{i+1} \in [0, t_{i+1}]$ and $s_{n+1} \in [0, T - \sum_{j=1}^n t_j]$,

$$\bigcup_{x \in K_i} \text{supp}\{Q(\varphi_{t_{i+1}}(x), \cdot)\} \subset K_{i+1}, \quad \varphi_{s_{i+1}}(K_i) \subset \tilde{K}, \quad \varphi_{s_{n+1}}(K_n) \subset \tilde{K}.$$

Assumption 1. *Durmus et al. (2021)[A3] The homogeneous characteristics (φ, λ, Q) satisfy*

1. the flow φ and the Markov kernel Q are compactly compatible;

2. $\lambda \in C^1(T\mathcal{M})$ and for all $f \in C^1(T\mathcal{M})$, $\lambda Q^\epsilon f \in C^1(T\mathcal{M})$ and there exists a locally bounded function $\Psi : T\mathcal{M} \rightarrow \mathbb{R}_+$ such that for all $x \in K$,

$$\lambda \|\nabla(Q^\epsilon f)(x)\| \leq \|\Psi\|_{\infty, K} \sup\{|f(y)| + \|\nabla f(y)\| : y \in \text{supp}\{Q^\epsilon(x, \cdot)\}\};$$

3. $(t, x) \mapsto \varphi_t(x) \in C^1(\mathbb{R}_+ \times T\mathcal{M})$ and for all compact $K \subset T\mathcal{M}$ and $t \geq 0$,

$$\sup\{\|\nabla\varphi_s(x)\| \mid s \in [0, t], x \in K\} < +\infty.$$

Proposition 4.1 (Feller and Core of Generator). *Let $(P_t)_{t \geq 0}$ be the transition semigroup of $(\varphi, \lambda_{ref}, Q^\epsilon)$ on $T\mathcal{M}$, where (\mathcal{M}, g) is a compact smooth Riemannian manifold and φ is the Hamiltonian flow associated to the Hamiltonian $H \in C^2(T\mathcal{M})$. Then, $(P_t)_{t \geq 0}$ is Feller and $C_c^1(T\mathcal{M})$ is a core for the strong generator of $(P_t)_{t \geq 0}$ seen as a semigroup on $C_0(T\mathcal{M})$.*

Proof. If we prove that $(\varphi, \lambda_{ref}, Q^\epsilon)$ satisfies assumption 1, then from Durmus et al. (2021)[Theorem 17] $(P_t)_{t \geq 0}$ satisfies the Feller property. Once the Feller property is established by Lemma 4.2 and due to the fact that $T\mathcal{M}$ is a complete metric space we have by Böttcher et al. (2013)[Lemma 1.4] strong continuity of $(P_t)_{t \geq 0}$ and that $(P_t)_{t \geq 0}$ is Feller. Further to this $C_c^1(T\mathcal{M})$ is a core for the strong generator of $(P_t)_{t \geq 0}$ seen as a semigroup on $C_0(T\mathcal{M})$ is a consequence of Durmus et al. (2021)[Theorem 17] and Ethier and Kurtz (1986)[Proposition 3.3, Chapter 1]. We will now establish Assumption 1.

For any compact set $K \subset T\mathcal{M}$, as K is compact, $|v|_g \leq M_K$ for some constant $M_K \geq 0$ and for all v such that $(\cdot, v) \in K$. Then by the same argument to that of Lemma 4.3, but choosing M_ϵ larger than M_K we have that all PDMPs starting in K are contained in a compact set \tilde{K} . We can define $K_0 = K$ and $K_i = \tilde{K}$ for all $i \geq 1$. Then we have the flow φ and Q_ϵ are compactly compatible and hence assumption 1i) holds.

We show assumption 1ii) as follows. Trivially we have $\lambda \in C^1(T\mathcal{M})$. We have taken the metric to be smooth and hence, as the truncated Gaussian distribution has a smooth transition kernel, we have that $Q^\epsilon f \in C^1(T\mathcal{M})$. Firstly we note that

$$\text{supp}\{Q^\epsilon(x, \cdot)\} = \{(x, v) \mid |v|_g \leq M(x)\},$$

which is compact by Lemma A.1. For all continuously differentiable functions $f : T\mathcal{M} \rightarrow \mathbb{R}$, with $(x, y) \in T\mathcal{M}$, we define

$$A(x, y) := \lambda_{ref} Q^\epsilon f(x, y) = \frac{\lambda_{ref}}{1 - \epsilon/2\lambda_{ref}} \int_{B(0, M(x))} f(x, y') \psi(x) (dy').$$

Therefore it is sufficient to show that for all compact sets $K \subset T\mathcal{M}$, and for all $(x, y) \in K$,

$$\|\nabla A(x, y)\| \leq \sup_{(w, z) \in K} \{\Psi(w, z)\} \sup\{|f|(x, y') + \|\nabla f(x, y')\| \mid |y'|_g \leq M(x)\},$$

where $\Psi : T\mathcal{M} \rightarrow \mathbb{R}$ is bounded on compact sets of $T\mathcal{M}$. Define $\|\cdot\|_{\infty, M(x)} \equiv \|\cdot\|_{\infty, B(0, M(x))}$. We have that for all $(x, y) \in T\mathcal{M}$, since all functions considered are C^1 and hence bounded

on all compact sets of $T\mathcal{M}$ we have the following computation which uses the dominated convergence theorem, a Leibniz's integral rule and a spherical coordinate system:

$$\begin{aligned}
\|\nabla A(x, y)\| &= \frac{\lambda_{ref}}{1 - \epsilon/2\lambda_{ref}} \|\nabla_x \int_{B(0, M(x))} f(x, y') \psi(x, y') dy'\| \\
&= C \|\nabla_x \int_0^{M(x)} \int_{S^{n-1}} f(x, r, \sigma) \psi(x, r, \sigma) r^{n-1} d\sigma dr\| \\
&= C \|\int_0^{M(x)} \int_{S^{n-1}} \nabla_x (f(x, r, \sigma) \psi(x, r, \sigma) r^{n-1}) d\sigma dr + \\
&\quad \int_{S^{n-1}} f(x, M(x), \sigma) \psi(x, M(x), \sigma) M(x)^{n-1} d\sigma \cdot \nabla_x M(x)\| \\
&\leq C \|\int_{B(0, M(x))} \nabla_x (f(x, y') \psi(x, y')) dy'\| + \\
&\quad C \|\int_{S^{n-1}} f(x, M(x), \sigma) \psi(x, M(x), \sigma) d\sigma\| \cdot \|M(x)^{n-1} \nabla_x M(x)\|_\infty \\
&\leq C_1 \|\int_{B(0, M(x))} \nabla_x (f(x, y')) \psi(x, y') dy'\| + \\
&\quad C_1 \|\int_{B(0, M(x))} f(x, y') \nabla_x (\psi(x, y')) dy'\| + C_2 \|f(x, \cdot)\|_{\infty, M(x)} \\
&\leq C_1 \|\nabla_x f(x, \cdot)\|_{\infty, M(x)} + C_2 \|f(x, \cdot)\|_{\infty, M(x)} + \\
&\quad C_3 \|f(x, \cdot)\|_{\infty, M(x)} \|\int_{B(0, M(x))} \nabla_x \psi(x, y') dy'\| \\
&\leq C_1 \|\nabla_x f(x, \cdot)\|_{\infty, M(x)} + C_2 \|f(x, \cdot)\|_{\infty, M(x)} + C_3 \|f(x, \cdot)\|_{\infty, M(x)} (M(x)^n) \\
&\leq C_1 \|\nabla f(x, \cdot)\|_{\infty, M(x)} + C_2 \|f(x, \cdot)\|_{\infty, M(x)} \\
&\leq (C_1 + C_2) \|\|\nabla f(x, \cdot)\| + |f(x, \cdot)|\|_{\infty, M(x)},
\end{aligned}$$

where C, C_1, C_2 and C_3 are general constants carrying line by line and ∇_x denotes the differential operator with respect to position on \mathcal{M} and we have bounded $\nabla_x \psi$ universally on $\{(x, y) \mid x \in \mathcal{M}, |y|_g \leq M(x)\} \subset T\mathcal{M}$. Therefore we have the required result by setting $\Psi = C_1 + C_2$. Finally we have to show assumption liii), where we use the fact that φ is continuously differentiable, when $U \in C^2(\mathcal{M})$ and for any compact set $K \subset T\mathcal{M}$ we have that $|v|_g \leq M_K$ for all $(x, v) \in T\mathcal{M}$. Then by the same argument as that of Lemma 4.3 we can define a larger constant such that all PDMPs starting in K have bounded velocity and hence are contained in a compact set \tilde{K} . Hence assumption liii) holds by the fact that a continuous function on a compact set is bounded. \square

Theorem 4.5 (RT-RMHMC Feller and Core). *Let $(P_t)_{t \geq 0}$ be the transition semigroup of $(\varphi, \lambda_{ref}, Q)$ on $T\mathcal{M}$, where (\mathcal{M}, g) is a compact smooth Riemannian manifold and φ is the Hamiltonian flow associated to the Hamiltonian $H \in C^1(T\mathcal{M})$. Then, $(P_t)_{t \geq 0}$ is Feller and $C_c^1(T\mathcal{M})$ is a core for the strong generator of $(P_t)_{t \geq 0}$ seen as a semigroup on $C_0(T\mathcal{M})$.*

Proof. By construction of Q^ϵ we have the property that

$$\sup_{x \in \mathcal{M}, A \in \mathcal{B}(\mathcal{M})} \{\lambda^\epsilon(x) \wedge \lambda(x) |Q^\epsilon(x, A) - Q(x, A)| + |\lambda^\epsilon(x) - \lambda(x)|\} \leq \epsilon.$$

Using Durmus et al. (2021)[Theorem 11], Proposition 4.1, Durmus et al. (2021)[Theorem 17] and the same argument as Durmus et al. (2021)[Theorem 21] we have the required result. \square

Corollary 4.5.1 (Invariant measure for RT-RMHMC). *Let $(P_t)_{t \geq 0}$ be the transition semi-group of $(\varphi, \lambda_{ref}, Q)$ on $T\mathcal{M}$, where (\mathcal{M}, g) is a compact smooth Riemannian manifold and φ is the Hamiltonian flow associated to the Hamiltonian $H \in C^2(T\mathcal{M})$. Let μ be the measure on $(T\mathcal{M}, \mathcal{B}(T\mathcal{M}))$ given by*

$$\mu(dz) \propto e^{-H(x,v)} d\lambda_{T\mathcal{M}}(z),$$

where $d\lambda_{T\mathcal{M}}$ is the Liouville measure of $T\mathcal{M}$. Then μ is invariant for RT-RMHMC.

5 Numerical Implementation and Metropolis-Hastings step

This section is based on Lee et al. (2017)[Chapter 3] and provides a brief introduction to Lagrangian and Hamiltonian dynamics with constraints.

Consider manifolds \mathcal{M} embedded in \mathbb{R}^n that can be described by algebraic equations

$$g_i(x) = 0, \quad i = 1, \dots, m,$$

where $g_i : \mathbb{R}^n \rightarrow \mathbb{R}$ $i = 1, \dots, m$ are continuously differentiable functions with linearly independent gradient functions for all $x \in \mathcal{M}$.

We refer to such a submanifold as an algebraic constraint manifold. We can express the Euler-Lagrange equations as an orthogonal projection of the Euler-Lagrange equations in \mathbb{R}^n onto the constraint manifold, hence we have

$$\frac{d}{dt} \left(\frac{\partial L(x, \dot{x})}{\partial \dot{x}} \right) - \frac{\partial L(x, \dot{x})}{\partial x} + \sum_{i=1}^m \lambda_i \frac{\partial g_i(x)}{\partial x} = 0,$$

where λ_i are Lagrange multipliers for each of the constraints. We can then define an augmented Lagrangian function $L^a : T^*M \times \mathbb{R}^m \rightarrow \mathbb{R}$ by

$$L^a(x, \dot{x}, \lambda) = L(x, \dot{x}) + \sum_{i=1}^m \lambda_i g_i(x).$$

Then the Euler-Lagrange equations can be expressed as

$$\frac{d}{dt} \left(\frac{\partial L^a(x, \dot{x}, \lambda)}{\partial \dot{x}} \right) - \frac{\partial L^a(x, \dot{x}, \lambda)}{\partial x} = 0$$

and the augmented Hamiltonian function $H^a : T^*\mathcal{M} \times \mathbb{R}^m \rightarrow \mathbb{R}$ as

$$H^a(x, \mu, \lambda) = \mu \cdot \dot{x} - L^a(x, \dot{x}, \lambda),$$

and we therefore obtain Hamilton's equations (see Hartmann (2007))

$$\begin{aligned}\dot{x} &= \frac{\partial H^a(x, \mu, \lambda)}{\partial \mu} \\ \dot{\mu} &= -\frac{\partial H^a(x, \mu, \lambda)}{\partial x}.\end{aligned}$$

We next introduce a new formulation of RT-RMHMC for constraint manifolds which we will use for numerical simulation. Note that a constraint manifold Hamiltonian Monte Carlo method was introduced in Brubaker et al. (2012), but with a deterministic duration parameter. We will use the same notation as that used in Brubaker et al. (2012) to introduce randomized time into this algorithm.

Let $\mathcal{M} := \{x \in \mathbb{R}^d \mid g_i(x) = 0, i = 1, \dots, m\} \subset \mathbb{R}^d$ be a constraint manifold and let $c(x) := (g_1(x), \dots, g_m(x))^T$. We want to simulate Hamiltonian dynamics subject to the constraint manifold, and let $C(x) = \frac{\partial c}{\partial x}$ denote the Jacobian of the constraints, which we assume to have full rank everywhere.

Define the Hamiltonian of the constrained system as

$$H(x, v) = U(x) + K(v),$$

where $K(v) = \frac{1}{2}v^T v$ is the kinetic energy. v lies in the cotangent space, $\mathcal{T}_x^* \mathcal{M} = \{v \mid C(x) \frac{\partial H}{\partial v}(x, v) = 0\}$, and the respective cotangent bundle is defined $\mathcal{T}^* \mathcal{M} = \{(x, v) \mid c(x) = 0 \text{ and } C(x) \frac{\partial H}{\partial v} = 0\}$.

The dynamics of the constrained system in terms of the Hamiltonian is thus given by

$$\begin{aligned}\dot{v} &= -\frac{\partial H}{\partial x} + C(x)^T \lambda, \\ \dot{x} &= \frac{\partial H}{\partial v}, \\ 0 &= c(x),\end{aligned}$$

where we remark that we can naturally identify the tangent and cotangent spaces and bundles.

If we let π be our target distribution with respect to the Lebesgue measure on \mathcal{M} and $\pi_{\mathcal{H}}$ with respect to the Hausdorff measure, and define our mass matrix to be the metric tensor of our constraint manifold, then we have exactly the RT-RMHMC with the Lagrange multipliers introduced to ensure our simulated dynamics stay on the tangent bundle. We also let $U(x) = -\log \pi_{\mathcal{H}}(x)$ be the potential energy of our constrained system. If we know $\pi_{\mathcal{H}}$ explicitly we can avoid computation of the metric tensor by assuming our system is isometrically embedded in Euclidean space. Under this assumption we can then consider the following explicit algorithm for simulation of Randomized time constrained Hamiltonian Monte Carlo and we will discuss and justify the embedding assumption further in section 5.2.

Algorithm 2: RT-CHMC

- Initialise x_0 arbitrarily on \mathcal{M} and sample $v_0 \sim \mathcal{N}(0, I \mid C(x_0)v_0 = 0)$.
- Initialise $t_0 = 0$.
- for $k = 1, 2, \dots$ do
 - Update time via $t_k = t_{k-1} + \delta t$, where $\delta t \sim \exp(1/\lambda)$.
 - Evolve over $[t_{k-1}, t_k]$ Hamilton's equations subject to constraints $c(\cdot)$ with initial condition $(x(t_{k-1}), v(t_{k-1})) = (x_{t_{k-1}}, v_{t_{k-1}})$ and Hamiltonian

$$H(x, v) = -\log \pi_{\mathcal{H}}(x) + \frac{1}{2}v^T v$$

- Set

$$(x_s, v_s) = (x(s), v(s)) \text{ for } s \in [t_{k-1}, t_k]$$

- Set $x_{t_k} = x(t_k)$.
 - Sample $v_{t_k} \sim \mathcal{N}(0, I \mid C(x_{t_k})v_{t_k} = 0)$
-

In this algorithm we sample the Gaussian distribution on the tangent space at a point on \mathcal{M} . We can do this by sampling a Gaussian distributed vector and then projecting this orthogonally. To orthogonally project a momentum vector onto $T^*\mathcal{M}$ and correctly resample the momentum in algorithm 2 at $x \in \mathcal{M}$ we apply the projector

$$P_{\mathcal{M}}(x) := I - C(x)^T (C(x)C(x)^T)^{-1} C(x).$$

Proposition 5.1. *If $v' \sim \mathcal{N}(0, I)$ then $v = P_{\mathcal{M}}(x)v'$ is distributed according to $v \sim \mathcal{N}(0, I \mid C(x)v = 0)$*

Proof. Can be found in Graham et al. (2021). □

5.1 Numerical Simulation

We use the RATTLE algorithm as a numerical solver for these constrained dynamics which was introduced in Andersen (1983) (see also Leimkuhler and Reich (2004)[Chapter 7]). It is a generalisation of the leapfrog integrator to handle constrained Hamiltonian dynamics. A step of the RATTLE algorithm consists of solving the following system of non-linear equations:

$$\begin{aligned} v_{n+1/2} &= v_n - \frac{h}{2} \left(\frac{\partial H(x_n, v_{n+1/2})}{\partial x} - C(x_n)^T \lambda_{(r)}^n \right), \\ x_{n+1} &= x_n + \frac{h}{2} \left(\frac{\partial H(x_n, v_{n+1/2})}{\partial v} + \frac{\partial H(x_n, v_{n+1/2})}{\partial v} \right), \\ 0 &= c(x_{n+1}), \\ v_{n+1} &= v_{n+1/2} - \frac{h}{2} \left(\frac{\partial H(x_{n+1}, v_{n+1/2})}{\partial x} - C(x_{n+1})^T \lambda_{(v)}^{n+1} \right), \\ 0 &= C(x_{n+1}) \frac{\partial H(x_{n+1}, v_{n+1})}{\partial v}, \end{aligned}$$

where $\lambda_{(r)}$ and $\lambda_{(v)}$ are the Lagrange multipliers associated to the constraints on the position and momentum at the end of each step and Δt is the step size. Then we have

$(x^{n+1}, v^{n+1}) \in T^*\mathcal{M}$. We solve these non-linear equations using Newton's method as described in Leimkuhler and Reich (2004) and discussed in Section 5.2.

5.2 Embedded Manifolds

We next introduce the theory of manifold embeddings as in Byrne and Girolami (2013) to show that numerical simulation of RT-CHMC is in fact simulation of RT-RMHMC on constraint manifolds.

If we know the form of the distribution $\pi_{\mathcal{H}}$ with respect to the Hausdorff measure, then we can avoid the computation of the metric tensor and the lack of a global coordinate system (Byrne and Girolami (2013)). We achieve this using isometric embeddings, remarking that every Riemannian manifold can be isometrically embedded in Euclidean space due to the Nash embedding theorem (Nash (1956)). If we have an isometric embedding $\xi : \mathcal{M} \rightarrow \mathbb{R}^n$, then considering a path $q(t)$ on \mathcal{M} , the path $x(t) = \xi(q(t))$ is such that

$$\dot{x}_i(t) = \sum_j \frac{\partial x_i}{\partial q_j} \dot{q}_j(t).$$

We can then transform the phase space (q, p) , where $\dot{q} = G^{-1}p$, to the embedded phase space (x, v) , such that

$$v = \dot{x} = XG(q)^{-1}p = X(X^T X)^{-1}p, \text{ where } X_{ij} = \frac{\partial x_i}{\partial q_j},$$

since $G = X^T X$ due to the fact that the embedding is isometric and preserves inner products. Now the Hamiltonian (eq 2) can be written in terms of these coordinates as

$$H(x, v) = -\log \pi_{\mathcal{H}}(x) + \frac{1}{2}v^T v.$$

When considering sampling of the velocities in Algorithm 1 and Algorithm 2, since $p \sim \mathcal{N}(0, G(q))$, it follows that

$$v_0 \sim \mathcal{N}(0, X(X^T X)^{-1}X^T),$$

where $X(X^T X)^{-1}X^T$ is the orthogonal projection onto the tangent space of the embedded manifold (Byrne and Girolami (2013)). Therefore we can sample from $\mathcal{N}(0, I)$ and project onto the tangent space to obtain a necessary sample. The Hamiltonian is thus expressed in a form which is independent of the metric (provided we know the density with respect to the Hausdorff measure). We now introduce the numerical integrator's (RATTLE) scheme Leimkuhler and Reich (2004)[Chapter 7]:

$$\begin{aligned} x_{n+1} &= x_n + \Delta t v_{n+1/2} \\ v_{n+1/2} &= v_n - \frac{\Delta t}{2} \nabla_x U(x_n) - \frac{\Delta t}{2} C(x_n)^T \lambda_{(r)}^n \\ &\text{such that } 0 = c(x_{n+1}) \\ v_{n+1} &= v_{n+1/2} - \frac{\Delta t}{2} \nabla_x U(x_{n+1}) - \frac{\Delta t}{2} C(x_{n+1})^T \lambda_{(v)}^{n+1} \\ &\text{such that } 0 = C(x_{n+1})v_{n+1}, \end{aligned}$$

where we solve for $\lambda_{(r)}^n$ and $\lambda_{(v)}^{n+1}$ at each iteration so that the iterates lie in the tangent bundle.

We solve for $\lambda_{(r)}^n$ (a non-linear system of equations) by cycling through the constraints, adjusting one multiplier at each iteration. Denote by C_i the i th row of C and we first initialise

$$Q := \bar{x}_{n+1} = x_n + \Delta t v_n - \frac{\Delta t^2}{2} \nabla_x U(x_n).$$

Next we cycle through the list of constraints one after another as follows: for each $i = 1, \dots, m$ compute

$$\Delta \Lambda_i := \frac{g_i(Q)}{C_i(Q) C_i(x_n)},$$

and update Q by

$$Q := Q - C_i(x_n)^T \Delta \Lambda_i$$

until $g_i(Q) < tol$ for all $i = 1, \dots, m$, where tol is a certain prescribed tolerance. Then we set $x_{n+1} = Q$ and have $x_{n+1} \in \mathcal{M}$ within the tolerance. (Note that other stopping criteria could be used (see Ortega and Rheinboldt (2000)).)

We solve for $\lambda_{(v)}^{n+1}$ by solving the linear system:

$$(C(x_n) C(x_n)^T) \lambda_{(v)}^n = C(x_n) \left(\frac{2}{\Delta t} v_{n-1/2} - \nabla_x U(x_n) \right).$$

Once the linear system has been solved we obtain $(x_{n+1}, v_{n+1}) \in T^* \mathcal{M}$.

Theorem 5.1. *Let \mathcal{M} be a constraint manifold. Let $H \in C^2(T\mathcal{M})$, the RATTLE numerical integrator of the Hamiltonian system defined by H in $T\mathcal{M}$ is symmetric, symplectic and of order 2. Further it respects the manifold constraints.*

Proof. Given in Leimkuhler and Skeel (1994). □

5.3 Metropolis Hastings Adjustment

Let $\Psi_{\Delta t}^L : T\mathcal{M} \rightarrow T\mathcal{M}$ be the numerical integrator defined by L steps of RATTLE with step size Δt . This integrator approximates the Hamiltonian dynamics. For theoretical purposes we will also define the map $N : T\mathcal{M} \rightarrow T\mathcal{M}$ which negates the momentum term i.e. $N(x, v) \equiv (x, -v)$. Note that this leaves the Hamiltonian invariant and due to the fact that the momentum is resampled this has no affect on the samples from $\pi_{\mathcal{H}}$. We will define the following Metropolised RT-RMHMC, where we sample $T \sim \exp \lambda$ and fix a maximum time length Δt_{\max} below the stability threshold of the numerical integrator. Then we choose the number of leapfrog steps L to be $\lceil T/\Delta t_{\max} \rceil$. Having chosen L in this way, we set $\Delta t = T/L \leq \Delta t_{\max}$. At each step we perform L RATTLE steps with stepsize Δt .

Algorithm 3: RT-CHMC with Metropolis-Hastings step

- Initialise Δt_{\max} within the stability threshold.
 - Initialise x_0 arbitrarily on \mathcal{M} and sample $v_0 \sim \mathcal{N}(0, I \mid C(x_0)v_0 = 0)$.
 - Initialise $t_0 = 0$.
 - for $k = 1, 2, \dots$ do
 1. Sample $v_{k-1} \sim \mathcal{N}(0, I \mid C(x_{k-1})v_{k-1} = 0)$.
 2. – Sample $T \sim \exp(\lambda)$.
 - Set $L = \lceil T/\Delta t_{\max} \rceil$ and $\Delta t = T/L$.
 - Set $(x^*, v^*) = \Psi(x_{k-1}, v_{k-1}) = N(\Psi_{\Delta t}^L(x_{k-1}, v_{k-1}))$.
 - Accept (x^*, v^*) with probability $\min\{1, \exp\{H(x, v) - H(x^*, v^*)\}\}$ and set $(x_k, v_k) = (x^*, v^*)$.
 - Otherwise $(x_k, v_k) = (x_{k-1}, v_{k-1})$.
-

Proposition 5.2. μ is invariant with respect to the Markov kernel proposed in the above algorithm. Further to this μ is reversible with respect to the second step in the Markov kernel.

Proof. Let P_1 be the Markov kernel corresponding to the first step. It is clear that re-sampling from the Gaussian measure on the tangent space keeps $\pi_{\mathcal{H}}$ invariant as it is independent and also keeps $\psi(x)$ invariant, and therefore keeps μ invariant.

Let P_2 be the Markov Kernel corresponding the second step (the combination of the sampling the time duration, deterministic step by Ψ and the Metropolis-Hastings accept-reject step. Let L be an arbitrary number of RATTLE steps we will check that μ is reversible with respect to P_2 and hence also invariant.

P_2 is reversible with respect to μ if for every measurable bounded function $f : T\mathcal{M} \times T\mathcal{M} \rightarrow \mathbb{R}$

$$\int \int f(z_1, z_2) \mu(dz_1) K(z_1, dz_2) = \int \int f(z_1, z_2) \mu(dz_2) K(z_2, dz_1).$$

For P_2 we have that $P_2(z_1, dz_2)$ is non-zero if and only if $z_2 = \Psi(z_1)$ and $z_2 = z_1$, hence we have that

$$\begin{aligned} \int \int f(z_1, z_2) \mu(dz_1) P_2(z_1, dz_2) &= \int \int f(z_1, \Psi(z_1)) \min[1, \exp(H(z_1) - H(\Psi(z_1)))] \mu(dz_1) + \\ &+ \int \int f(z_1, z_1) (1 - \min[1, \exp(H(z_1) - H(\Psi(z_1)))] \mu(dz_1). \end{aligned}$$

Now let $z_2 = \Psi(z_1)$, then due to the momentum reversal map N , we have that $z_1 = \Psi(z_2) = \Psi(\Psi(z_1))$, and by the volume preserving property of Ψ (preserving the Liouville measure), we have that

$$\mu(dz_2) = \mu(dz_1) \cdot \frac{\exp(-H(z_2))}{\exp(-H(z_1))} = \mu(dz_1) \cdot \exp(H(z_1) - H(z_2)),$$

and using this property we have that the first part of the above sum can be written as

$$\begin{aligned}
& \int \int f(z_1, \Psi(z_1)) \min [1, \exp (H(z_1) - H(\Psi(z_1)))] \mu(dz_1) \\
&= \int \int f(\Psi(z_2), z_2) \min [1, \exp (H(\Psi(z_2)) - H(z_2))] \cdot \exp (H(z_2) - H(\Psi(z_2))) \mu(dz_2) \\
&= \int \int f(\Psi(z_2), z_2) \min [1, \exp (H(z_2) - H(\Psi(z_2)))] \mu(dz_2).
\end{aligned}$$

Now considering the second part of the sum, through a change of variables and combining these two equations we have the required result. We therefore have that μ is reversible with respect to P_2 and by the same argument and considering f to be the identity we have invariance P_2 with respect to μ . Due to the fact that this calculation was independent of time we have that μ is invariant with respect to the Markov kernel of this algorithm. \square

We will now prove ergodicity under the following two assumptions by the same technique as Brubaker et al. (2012) and restating some of their results.

Assumption 2. Let $\mathcal{M} \in \{x \in \mathbb{R}^n \mid c(x) = 0\}$ be Riemannian manifold which is connected, smooth and differentiable. We assume that $\partial c / \partial x$ is full rank everywhere.

Assumption 3. Let \mathcal{M} be a Riemannian manifold which satisfies assumption 2. For $x \in \mathcal{M}$ we define $\mathcal{B}_r(x) = \{x' \in \mathcal{M} \mid d(x', x) \leq r\}$ to be the geodesic ball of radius r of x . We assume that there exists a $r > 0$ such that for every $x \in \mathcal{M}$ and $x' \in \mathcal{B}_r(x)$ there exists a unique choice of Lagrange multipliers and velocity $v \in T_x \mathcal{M}$, $v' \in T_{x'} \mathcal{M}$ for which $(v', x') = \Psi_{\Delta t}^L(v, x)$ for sufficiently small Δt .

Theorem 5.2 (Accessibility). Let $U \in C^2(\mathcal{M})$, and assuming assumption 2. For any $x_0, x_1 \in \mathcal{M}$ and Δt sufficiently small, there exists finite $v_0 \in T\mathcal{M}$, $v_1 \in T\mathcal{M}$ and Lagrange multipliers λ_0, λ_1 such that $(v_1, x_1) = \Psi_{\Delta t}(v_0, x_0)$.

Proof. Found in Brubaker et al. (2012)[Theorem 2] and is an extension of the results of Marsden and West (2001)[Theorem 2.1.1] and Hairer et al. (2006)[Theorem 5.6, Section IX.5.2]. \square

Theorem 5.3 (μ -irreducible). Let $U \in C^2(\mathcal{M})$, and under assumptions 2 and 3 we have that for any $x \in \mathcal{M}$, and measurable set $A \subset \mathcal{M}$ with positive measure. Then there exists an $n \in \mathbb{N}$ such that

$$K^n(x, A) > 0,$$

where K denotes the marginal transition kernel defined on \mathcal{M} of algorithm 3.

Proof. Based on Brubaker et al. (2012)[Theorem 3]. Fix $\Delta t > 0$ sufficiently small such that our assumption holds. For a measurable set $A \subset \mathcal{M}$, we can say A is contained in a compact set K , which can be covered by $\{B_{r/2}(x) \mid x \in K\}$. Then we have that for some $x' \in K$, $B_{r/2}(x') \cap A$ has positive measure. We can connect x and x' by a sequence of points $x_0, \dots, x_i, \dots, x_n$ for $0 \leq i \leq n$, defined on the geodesic between $x_0 = x$ and $x_n = x'$ such that $d(x, x_n) \leq r/2$. We can find unique v_0, \dots, v_n such that $(x_{i+1}, v_{i+1}) = \Psi_{\Delta t}^L(x_i, v_i)$ by Theorem 5.2. We have that

$$K(x_i, x_{i+1}) > 0$$

due to the Theorem 5.2 and the fact that $\phi(x_i)(v_i) > 0$. Considering the final step we have due to the triangle inequality $|x_{n-1} - \tilde{x}| < r$ for all $\tilde{x} \in B_{r/2}(x') \cap A$. Hence by the same reasoning and Theorem 5.2 we have that $K(x_{n-1}, \tilde{x}) > 0$ for all $\tilde{x} \in B_{r/2}(x') \cap A$. Using the fact that $K(x_i, x_{i+1}) > 0$ for all $0 \leq i \leq n-2$, and $K(x_{n-1}, \tilde{x}) > 0$ for all $\tilde{x} \in B_{r/2}(x') \cap A$ we have that $K^n(x, \tilde{x}) > 0$ for all $\tilde{x} \in B_{r/2}(x') \cap A$ and

$$K^n(x, A) \geq K^n(x, B_{r/2}(x') \cap A) = \int_{B_{r/2}(x') \cap A} K^n(x, y) \sigma_{\mathcal{M}}(dy) > 0.$$

□

Lemma 5.4 (Aperiodic). *Let $U \in C^2(\mathcal{M})$ and under assumptions 2 and 3 Algorithm 3 is aperiodic.*

Proof. Proof given in Brubaker et al. (2012)[Lemma 1].

□

Theorem 5.5 (Ergodicity). *Let $U \in C^2(\mathcal{M})$ and under assumptions 2 and 3 we have for μ -almost all starting values x*

$$\lim_{t \rightarrow \infty} \int_{\mathcal{M}} |K^t(x, y) - \pi_{\mathcal{H}}(y)| \sigma_{\mathcal{M}}(dy).$$

Proof. Since Algorithm 3 is μ -invariant by Theorem 5.2, μ -irreducible by Theorem 5.3 and aperiodic by Theorem 5.4 we have that the required result holds by Tierney (1994)[Theorem 1].

□

Remark 5.6. *We remark that with our framework we can deal with sampling on manifolds with boundary or manifolds with inequality constraints like that of the form*

$$S_+^2 := \{x \in \mathbb{R}^3 \mid |x|^2 - 1 = 0 \text{ and } x_3 > 0\}$$

by having an additional rejection condition in the Metropolis-Hastings step. This condition simply rejects samples which do not satisfy the inequality constraint. For example samples for which $x_3 \geq 0$.

Remark 5.7. *We also remark that for large choices of step size Δt it has been shown that $\Phi_{\Delta t}^L$ is not reversible for RATTLE, see Lelièvre et al. (2019); Zappa et al. (2018). In Lelièvre et al. (2019) they propose a method to combat this by having a reversibility check incorporated into the Metropolis-Hastings adjustment. In statistical and molecular dynamics applications such checks are not typically performed because it is implicitly assumed that Δt is sufficiently small to avoid non-reversible artifacts. However their method is compatible with our framework.*

6 Numerical results

We will perform numerical simulations of the RT-RMHMC algorithm and compare it to the RMHMC algorithm of Brubaker et al. (2012); Girolami and Calderhead (2011), specifically

exploring the underlying dynamics of the two processes. MCMC schemes are used to approximate expected values of certain functions f over some distribution with pdf π

$$\mathbb{E}_\pi(f) = \int f(x)\pi(x)dx,$$

where we can estimate this quantity using our MCMC scheme by

$$\bar{f} := \mathbb{E}_\pi(f) \approx \frac{1}{M} \sum_{i=1}^M f(X^i),$$

where X^i are the Markov chain from our MCMC method. We quantify the convergence rate associated to approximation of $\mathbb{E}_\pi(f)$ by considering the integrated autocorrelation function.

6.1 Integrated Autocorrelation and ESS

If the MCMC method converges quickly, we have that the variance $\sigma^2(\bar{f})$ (the variance of the estimator) is small. From the central limit theorem we know that as $N \rightarrow \infty$,

$$\sqrt{N}(\bar{f} - \langle f \rangle) \sim \mathcal{N}(0, a^2)$$

and hence

$$\lim_{N \rightarrow \infty} \sigma^2(\bar{f}) = \frac{a^2}{N},$$

where the quantity a is known as the asymptotic variance. We have the following result

$$a^2 = \tau_f \sigma^2(f),$$

where $\sigma^2(f)$ is the variance of f under the distribution π and is independent of the MCMC scheme used (see Casella (2004)[Chapter 12] for an in depth study).

We also have

$$\tau_f = 1 + 2 \sum_{i=1}^{\infty} \mathbf{corr}(f(X^0), f(X^i)),$$

which is known as the integrated autocorrelation (IAC). If all samples are independent, then $\tau_f = 1$. MCMC schemes generate correlated samples, thus $\tau_f > 1$.

The IAC (τ_f) is a measure of how dependent the samples are and the closer this value is to 1, the higher the quality of the MCMC samples produced. Note that we will use X^\bullet to denote the random variables in a Markov chain and X_\bullet to denote the outputs of an MCMC scheme. In the following numerics we approximate the IAC by a Monte Carlo method, that is we create a finite chain $\{f_n\}_{n=1}^N = \{f(X_i)\}_{n=1}^N$ from the MCMC schemes we want to test. We estimate

$$\mathbf{corr}(f(X^0), f(X^i)) \approx \frac{c_f(i)}{c_f(0)},$$

where

$$c_f(i) = \frac{1}{N-i} \sum_{n=1}^{N-i} (f_n - \mu_f)(f_{n+i} - \mu_f)$$

and

$$\mu_f = \frac{1}{N} \sum_{n=1}^N f_n.$$

We have that

$$\tau_f \approx 1 + 2 \sum_{i=1}^M \frac{c_f(i)}{c_f(0)},$$

for some large M such that $M \ll N$. Note that in practice one uses a fast Fourier transform method to calculate $c_f(\cdot)$ as it is much more computationally efficient.

We now define an additional metric of quality of samples known as effective sample size (ESS) which is defined as

$$N_{\text{eff}} = \frac{N}{\tau_f}$$

for a sample size of size N . This metric is used to say that a sample of size N of an MCMC algorithm has the efficiency of N_{eff} independent samples for computing the Monte Carlo average of f .

6.2 g-BAOAB

As a comparison method we implemented the g-BAOAB integrator of Leimkuhler and Matthews (2016), a numerical integrator for constrained underdamped Langevin dynamics. Constrained underdamped Langevin dynamics can be described by

$$\begin{aligned} \dot{x} &= v \\ \dot{v} &= -\nabla_x U(x) - \gamma v + \sqrt{2\gamma} R(t) - C(x)^T \lambda, \\ \text{such that } 0 &= c(x), \\ \text{and } 0 &= C(x)v, \end{aligned}$$

where γ is a friction coefficient and $R(t)$, is a vector-valued, stationary, zero-mean Gaussian process. The numerical integrator g-BAOAB is a splitting method for such dynamics, which uses similar constrained integrators as that of RT-RMHMC. We note that g-BAOAB is a biased sampling algorithm due to the error in the numerical integrator. For a full description of g-BAOAB and a discussion of the sampling error we refer to Leimkuhler and Matthews (2016).

6.3 Test Examples

We next provide examples of distributions on implicitly defined manifolds embedded in Euclidean space, with the distributions defined with respect to the Hausdorff measure of the manifold. We will consider two types of constraint manifolds: spheres and Stiefel manifolds.

Bingham-Von Mises-Fisher distribution on S^n

The first test case is the Bingham-Von Mises-Fisher (BVMF) distribution defined on the n -dimensional sphere embedded in \mathbb{R}^{n+1} , that is $S^n := \{x \in \mathbb{R}^{n+1} \mid \sum_{i=1}^{n+1} x_i^2 = 1\}$. The

BVMF distribution is the exponential family on $S^n \subset \mathbb{R}^{n+1}$ with density of the form

$$\pi_{\mathcal{H}}(x) \propto \exp \{c^T x + x^T A x\},$$

where $c \in \mathbb{R}^{n+1}$ and $A \in M_{n+1}(\mathbb{R})$ is a symmetric matrix. For a first test we chose

$$A = \text{diag}(-1000, 0, 1000), \quad c = (100, 0, 0).$$

We compare the IAC of $-\log \pi_{\mathcal{H}}$ of the RT-RMHMC method to that of the RMHMC method introduced in Girolami and Calderhead (2011). We compare methods by setting the event rate parameter λ of RT-RMHMC to be the deterministic duration parameter of RMHMC (running the dynamics for this duration before momentum randomization). We then compute the integrated autocorrelation of $-\log \pi_{\mathcal{H}}$ for the two methods for varying choices of λ by a Monte Carlo averaging procedure as described in section 6.1. The results are presented in Figure 1. Note we choose the step size in RATTLE to be $\Delta t = 0.001$ and sample $N = 1,000,000$ events with a burn time of 10% of samples before we compute the Monte Carlo average. We also use lags of up to $M = N/50$, 2 percent of the number of samples used to estimate the IAC.

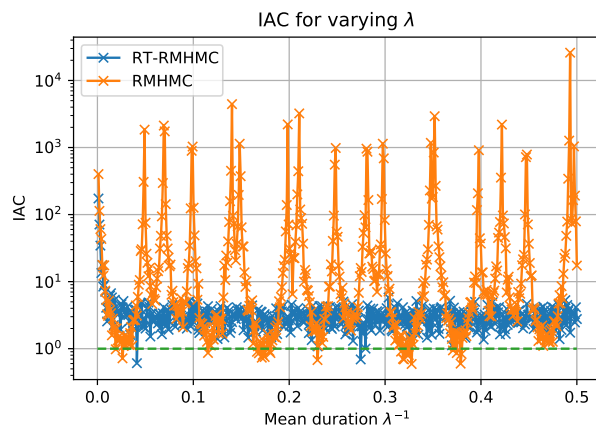


Figure 1: IAC estimates of $-\log \pi_{\mathcal{H}}$ for different choices of λ for the BVMF distribution with parameters $A = \text{diag}(-1000, 0, 1000)$ and $c = (100, 0, 0)$. λ is the deterministic duration parameter in RMHMC and the event rate in RT-RMHMC. The results are presented on a log scale with the green dashed line showing the IAC for independent samples.

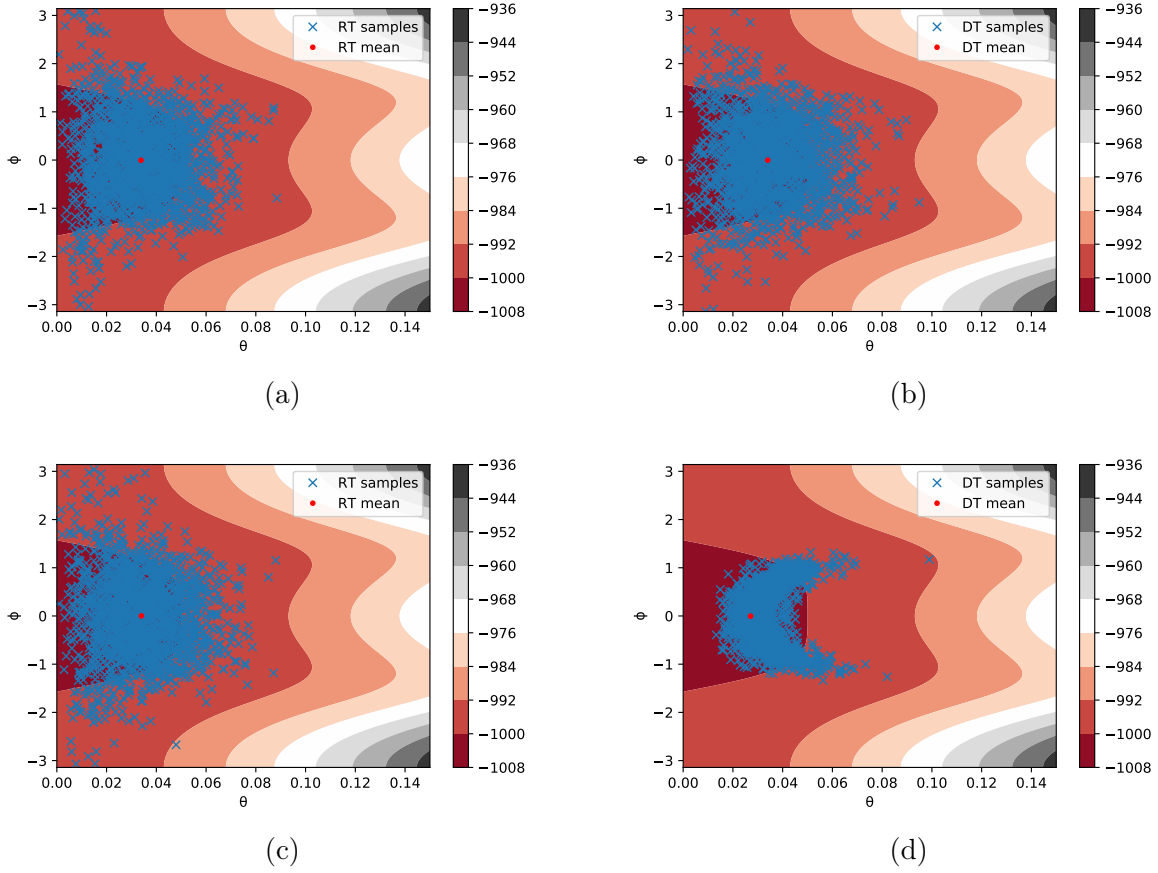


Figure 2: Contour plot of $-\log \pi_{\mathcal{H}}$ for the BVMF distribution with parameters $A = \text{diag}(-1000, 0, 1000)$ and $c = (100, 0, 0)$. The axis being a 2D parameterisation of S^2 . The points are 2000 samples after a 8000 sample burn in time from Randomized Time Riemannian Hamiltonian Monte Carlo and Riemannian Hamiltonian Monte Carlo for $\lambda^{-1} = 0.09$ and $\lambda^{-1} = 0.1$. Upper left: RT-RMHMC for $\lambda^{-1} = 0.09$. Upper right: RMHMC for $\lambda^{-1} = 0.09$. Lower left: RT-RMHMC for $\lambda^{-1} = 0.1$. Lower right: RMHMC for $\lambda^{-1} = 0.1$.

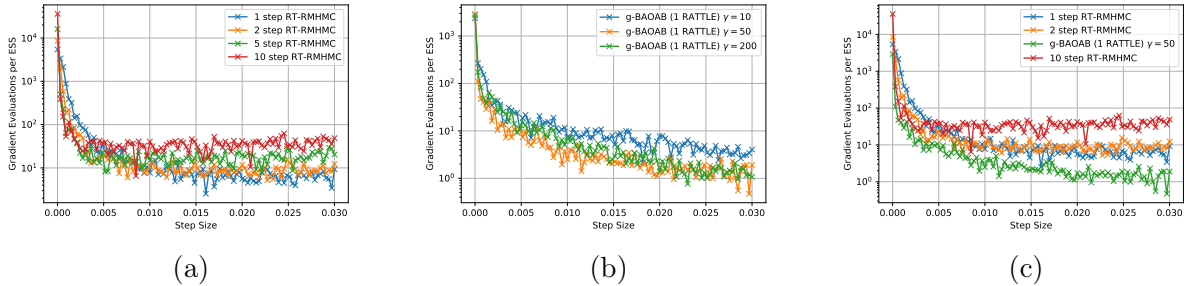


Figure 3: Gradient evaluation per ESS estimates of $-\log \pi_{\mathcal{H}}$ for the BVMF distribution with parameters $A = \text{diag}(-1000, 0, 1000)$ and $c = (100, 0, 0)$ and for varying choices of step-size. The legend denotes estimates for RT-RMHMC with different numbers of expected leapfrog steps. The legend for g-BAOAB illustrates different choices of friction parameter γ . These estimates are taken from 100,000 samples. Left: RT-RMHMC. Middle: g-BAOAB. Right: g-BAOAB and RT-RMHMC.

In our first example and Figure 1 we can see that the regularity of the quality of samples with respect to the duration parameter is poor when a deterministic duration parameter is used and nearly uniform across a wide interval for a Randomized duration with the same expected value. This is illustrated in Figure 2, where a small change in duration parameter causes the dynamics dramatically slows convergence and due to very slow mixing.

We next compare the efficiency of the method with the g-BAOAB constrained Langevin integrator, we find in figure 3 that g-BAOAB outperforms RT-RMHMC for large choices of the friction parameter γ (for this example $\gamma = 50$). g-BAOAB has no Metropolis-Hastings adjustment and hence is a biased sampling method. The bias in the samples creates errors in computed observables. For large choices of γ , this bias is dramatically reduced, but use of high friction may slow convergence of metastable systems. To explore this we next consider a bimodal distribution from Byrne and Girolami (2013).

We consider the Bingham-von Mises-Fisher distribution on S^4 with parameters:

$$A = \text{diag}(-20, -10, 0, 10, 20), \quad c = (40, 0, 0, 0, 0).$$

We compare a Monte Carlo running average of $U = -\log \pi_{\mathcal{H}}$ with $N = 4 \times 10^6$ for different choices of Δt and compare 10-step RT-RMHMC to g-BAOAB, with $\gamma = 2$, a relatively large friction parameter for such a system. It is shown in Figure 4 that g-BAOAB incurs bias for large step sizes and convergence is slow for large choices of the friction parameter for this metastable system. The Figure also shows that this is not the case for RT-RMHMC.

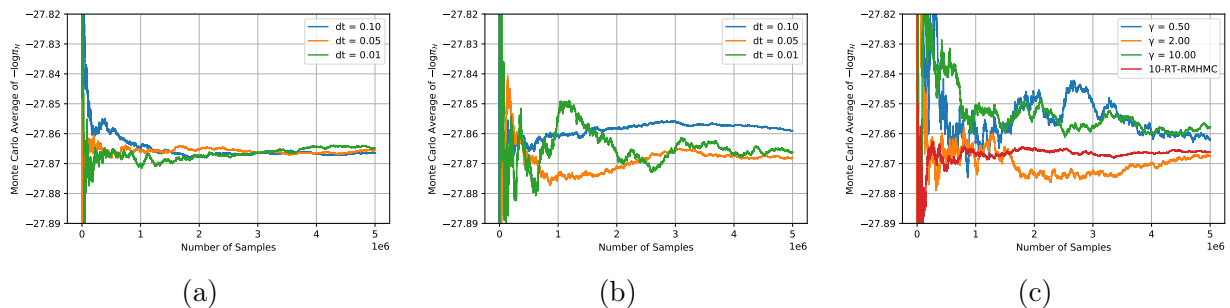


Figure 4: Monte Carlo Average of $-\log \pi_{\mathcal{H}}$ for the BVMF distribution with parameters $A = \text{diag}(-20, -10, 0, 10, 20)$ and $c = (40, 0, 0, 0, 0)$ with $N = 5 \times 10^6$ samples. Comparing 10-step RT-RMHMC with g-BAOAB. Left: 10 step RT-RMHMC. Middle: g-BAOAB with $\gamma = 2$. Right: g-BAOAB with $dt = 0.01$

Von Mises-Fisher distribution on $\mathbb{V}_{d,p}$

Def 6.1. A Stiefel manifold $\mathbb{V}_{d,p}$ is the set of $d \times p$ matrices X such that $X^T X = I$.

These arise in many statistical problems which are discussed in Byrne and Girolami (2013). Applications include dimensionality reduction such as is used in factor analysis, principal component analysis (Jolliffe (1986)) and directional statistics (Mardia et al. (2000)). These are a generalisation of orthogonal groups.

The von Mises-Fisher distribution on Stiefel manifolds is defined by the density

$$p_{vMF}(X) \propto \exp(\text{Tr}(F^T X)) = \exp(\langle f_1, x_1 \rangle + \dots + \langle f_p, x_p \rangle),$$

where x_i and f_i are the columns of F and X .

We consider the skew-symmetric matrix

$$A := \begin{pmatrix} 0 & 2 & -45 \\ -2 & 0 & -4 \\ 45 & 4 & 0 \end{pmatrix}$$

for $\mathbb{V}_{3,3} = O(3)$ and we also consider a larger example where $F = [I, -A, I, -A, I, -A]^T \in \mathbb{V}_{18,3}$. We simulate IAC estimates for these two distributions for varying duration parameters. In the simulations we use a step size of $\Delta t = 0.001$ and 100,000 samples in each IAC estimate. The results are shown in Figure 5.

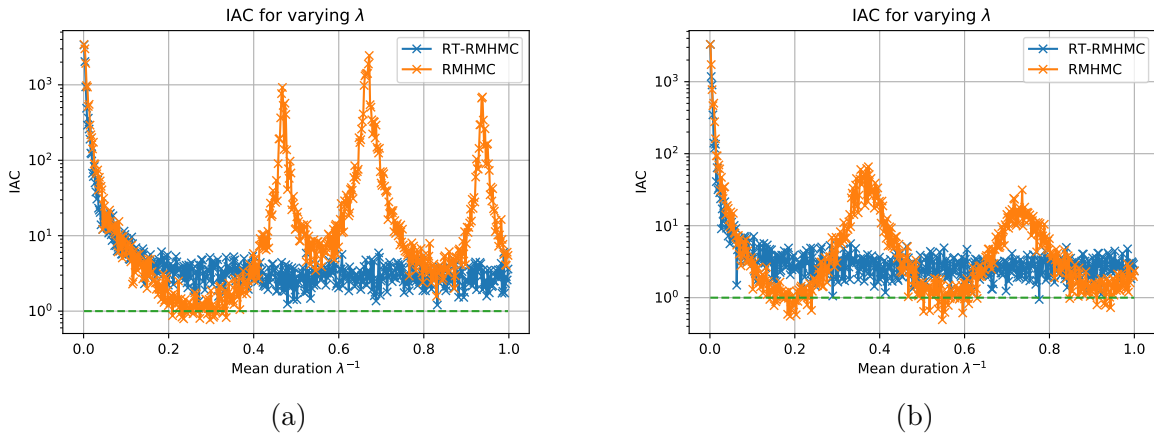


Figure 5: IAC estimates of $-\log \pi_{\mathcal{H}}$ for different choices of event rate λ for the VMF distribution on $O(3)$ and $\mathbb{V}_{18,3}$ with parameters given in the captions. Left: VMF distribution on $O(3)$ with parameters $F = \text{Skew}(2, -45, -4)$. Right: VMF distribution on $\mathbb{V}_{18,3}$ with parameters $F = [I, -A, I, -A, I, -A]^T$.

6.4 High Dimensional Covariance Estimation

In many statistical applications for analysing high dimensional data sets it is necessary to estimate sample covariances. This can be challenging when the number of dimensions is larger than the number of data points, as the sample covariance estimator does not work well in such cases. Lam (2020) provides a review of high-dimensional covariance estimation and applications in principal component analysis (Shen et al. (2016)), cosmological data analysis (Joachimi (2017)) and finance (Lam (2016)). Lam (2020) focuses on the set up where the matrix dimension is diverging or even larger than the sample size. In this setting one needs to estimate the population covariance matrix Σ of a set of n , p -dimensional data vectors, which we assume are drawn from an underlying distribution.

One estimator is the sample covariance matrix, which is defined by $\Sigma_S = 1/n \sum_{i=1}^n (\mathbf{x}_k - \bar{\mathbf{x}})(\mathbf{x}_k - \bar{\mathbf{x}})^T$, where $\bar{\mathbf{x}} = 1/n \sum_{k=1}^n \mathbf{x}_k$ is the sample mean. However this is a poor estimator of Σ when p is large compared to the sample size n (due to rank deficiency). A way to combat this is to consider regularised covariance matrix estimators which include structural assumptions on the covariance matrix Σ .

One such method which has been proposed assumes the structure of a low rank matrix plus a sparse matrix (see Ross (2013) and Lam (2020)). This structure is known as a spiked covariance structure and has been studied in Bouchard et al. (2020), Lam (2020) and Cai et al. (2015). There have been interesting applications to finance (Fan et al. (2008)), chemometrics (Kritchman and Nadler (2008)), and astronomy (Joachimi (2017)). The covariance matrix Σ is assumed to be expressible in the form

$$\Sigma = XD_1X^T + D_2,$$

where X is a Stiefel manifold of dimension $p \times m$ for $p \gg m$ and D_i for $i = 1, 2$ are diagonal matrices of dimensions $m \times m$ and $p \times p$ respectively. The motivation for this structure is that we assume that lower dimensional variables \mathbf{y}_i can describe the data \mathbf{x}_i such that

$$\mathbf{x}_i = X\mathbf{y}_i + \boldsymbol{\epsilon}_i,$$

where X is a $p \times m$ matrix with orthogonal columns. We have that

$$\Sigma = X\Sigma_y X^T + \Sigma_\epsilon,$$

which we interpret as a low rank matrix (rank m) plus a sparse matrix. We take Σ_y and Σ_ϵ to be diagonal, which is an approximation of the spiked covariance structure Chamberlain and Rothschild (1982).

Assume a uniform prior on X with respect to the Hausdorff measure on X . Further assume a half-normal prior of the diagonal entries of D_i for $i = 1, 2$ to ensure positive definiteness. We also consider the following likelihood for the covariance estimation

$$\mathcal{L}(\Sigma \mid \mathbf{x}_1, \dots, \mathbf{x}_p) = (2\pi)^{-np/2} \prod_{i=1}^n \det(\Sigma)^{-1/2} \exp\left(-\frac{1}{2}(\mathbf{x}_i - \bar{\mathbf{x}})^T \Sigma^{-1}(\mathbf{x}_i - \bar{\mathbf{x}})\right).$$

Introduce the posterior distribution

$$p(\Sigma \mid \mathbf{x}_1, \dots, \mathbf{x}_p) \propto \mathcal{L}(\Sigma \mid \mathbf{x}_1, \dots, \mathbf{x}_p)p(\Sigma),$$

where $p(\Sigma) = p(X)p(D_1)p(D_2)$ for $X \sim \mathcal{U}(\mathbb{V}_{p,m})$, $D_{1jj} \sim \mathcal{N}_+(0, \sigma_1^2)$ for $j = 1, \dots, m$ and $D_{2jj} \sim \mathcal{N}_+(0, \sigma_2^2)$ for $j = 1, \dots, p$ and \mathcal{N}_+ denotes the half-normal distribution. Define the potential $U : \mathbb{V}_{p,m} \times \mathbb{R}^m \times \mathbb{R}^p \mapsto \mathbb{R}$ by

$$U(X, \mathbf{d}_1, \mathbf{d}_2) = -\log \mathcal{L}(\Sigma(X, \mathbf{d}_1, \mathbf{d}_2) \mid \mathbf{x}_1, \dots, \mathbf{x}_p) - \log p(X) - \log p(\mathbf{d}_1) - \log p(\mathbf{d}_2)$$

with forces given by

$$\frac{\partial U}{\partial X_{ij}} = \frac{\partial U}{\partial \Sigma_{kl}} \frac{\partial \Sigma_{kl}}{\partial X_{ij}} = \left(\frac{1}{2} n (\Sigma^{-1})_{kl}^T + \frac{1}{2} \sum_{r=1}^n (\mathbf{x}_r - \bar{\mathbf{x}})^T B^{kl} (\mathbf{x}_r - \bar{\mathbf{x}}) \right) \frac{\partial \Sigma_{kl}}{\partial X_{ij}},$$

where $[B^{kl}]_{ij} = -(\Sigma^{-1})_{ik}(\Sigma^{-1})_{lj}$ and

$$\frac{\partial \Sigma_{kl}}{\partial X_{ij}} = \begin{cases} X_{kj} D_{jj}^1 & k \neq i, l = i, \\ D_{jj}^1 X_{lj} & k = i, l \neq i, \\ 2X_{ij} D_{jj}^1 & k = i, l = i, \\ 0 & \text{otherwise.} \end{cases}$$

We also have that

$$\frac{\partial U}{\partial d_{ij}} = \frac{\partial U}{\partial \Sigma_{kl}} \frac{\partial \Sigma_{kl}}{\partial d_{ij}} + \frac{d_{ij}}{\sigma_1^2},$$

for $i = 1, 2$ and where

$$\frac{\partial \Sigma_{kl}}{\partial d_{1j}} = X_{kj} X_{lj}$$

for $j = 1, \dots, m$ and

$$\frac{\partial \Sigma_{kl}}{\partial d_{2j}} = \begin{cases} 1 & \text{if } k = l = j \\ 0 & \text{otherwise} \end{cases}$$

for $j = 1, \dots, p$. We will use the likelihood and its gradient for implementing our RT-RMHC algorithm for such models.

Covariance estimation for cosmological data

We consider an application of high dimensional covariance estimation in cosmological data analysis introduced in Joachimi (2017) and discussed in Lam (2020). The data consists of $p = 120$ and $n = 2000$ independent and identically distributed data vectors and comes from a mock cosmological survey analyzed in Joachimi (2017). We then consider a subsample of this data of $n = 80$ data vectors and use the sparse covariance estimation method we introduced with RT-RMHMC as a sampling method. We will compare this method with the sample covariance matrix with $n = 80$ samples. The performance of RT-RMHMC based covariance estimation is first shown on a toy example from Joachimi (2017). The data consists of $n = 2000$ independent and identically distributed data vectors, where each vector of size $p = 120$'s first half are sampled from a Gaussian distribution with mean 0 and variance 5 and the second half from a Gaussian distribution with mean 0 and variance 1 with the results shown in Figure 6.

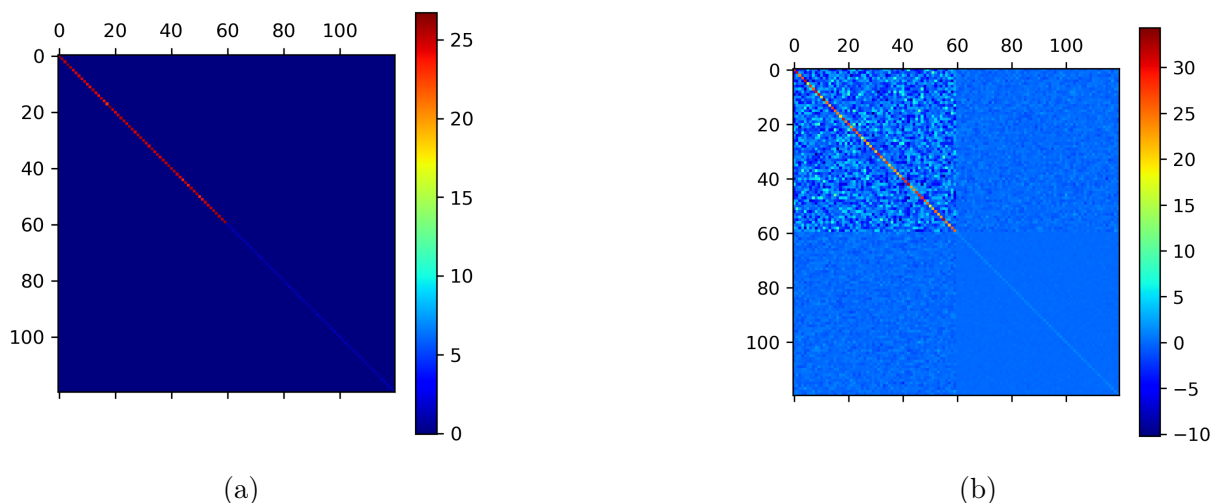


Figure 6: Covariance estimates of toy data of 120-dimensional data vectors. Σ_S is a sample covariance using 80 data points and $\hat{\Sigma}$ is a Bayesian estimation of Σ using 80 data points. The Bayesian estimation uses priors of $\sigma_1 = 25$ and $\sigma_2 = 100$ after normalisation and 50,000 samples from RT-RMHMC. Left: $\hat{\Sigma}$. Right: Σ_S .

6.4.1 Data

We now provide an example of using RT-RMHMC for high-dimensional covariance estimation for real data. The data is taken from Joachimi (2017) and consists of covariances of two-point correlation functions of cosmic weak lensing. It is simulated using coupled log-normal random fields from angular power spectra. For further information we refer the reader to Joachimi (2017). We will test this method using $2n/3$ data vectors, where n is the dimension of the data vectors. Therefore we are in the setting where the dimension of the covariance matrix is larger than the number of samples. For our low rank plus sparse structure we choose $m = p/6 \ll p$ and to ensure fast convergence we will normalize the data entry-wise and initialise our Markov chain via a eigenvalue decomposition of the sample covariance. We initialise our Markov chain as

$$\Sigma_0 = X^T D_1 X + D_2 \approx \Sigma_S,$$

using the sample covariance matrix Σ_S and where D_2 is the diagonal of Σ_S and $X^T D_1 X$ corresponds to the eigenvalue decomposition of $\Sigma_S - D_2$, but with the p largest eigenvectors. After the covariance of the normalized data is estimated it can easily be rescaled to match the real data via entry-wise multiplication with the outer product of the entry-wise standard deviations. We compare our method to a maximum a posteriori (MAP) estimate of the covariance matrix which uses a simple constrained gradient descent algorithm with Lagrange multipliers to ensure that the “low-rank plus sparse” structure is maintained. We compare the Bayesian and MAP approaches using a relative Frobenius norm and a covariance metric introduced by Förstner and Moonen (2003) which is defined by

$$d(A, B) = \sqrt{\sum_{i=1}^n \ln^2 \lambda_i(A, B)},$$

where A and B are covariance matrices and $\lambda_i(A, B)$ are the generalized eigenvalues from $\det(\lambda A - B) = 0$. As pointed out in Förstner and Moonen (2003), this covariance metric is affine invariant and invariant to inversion.

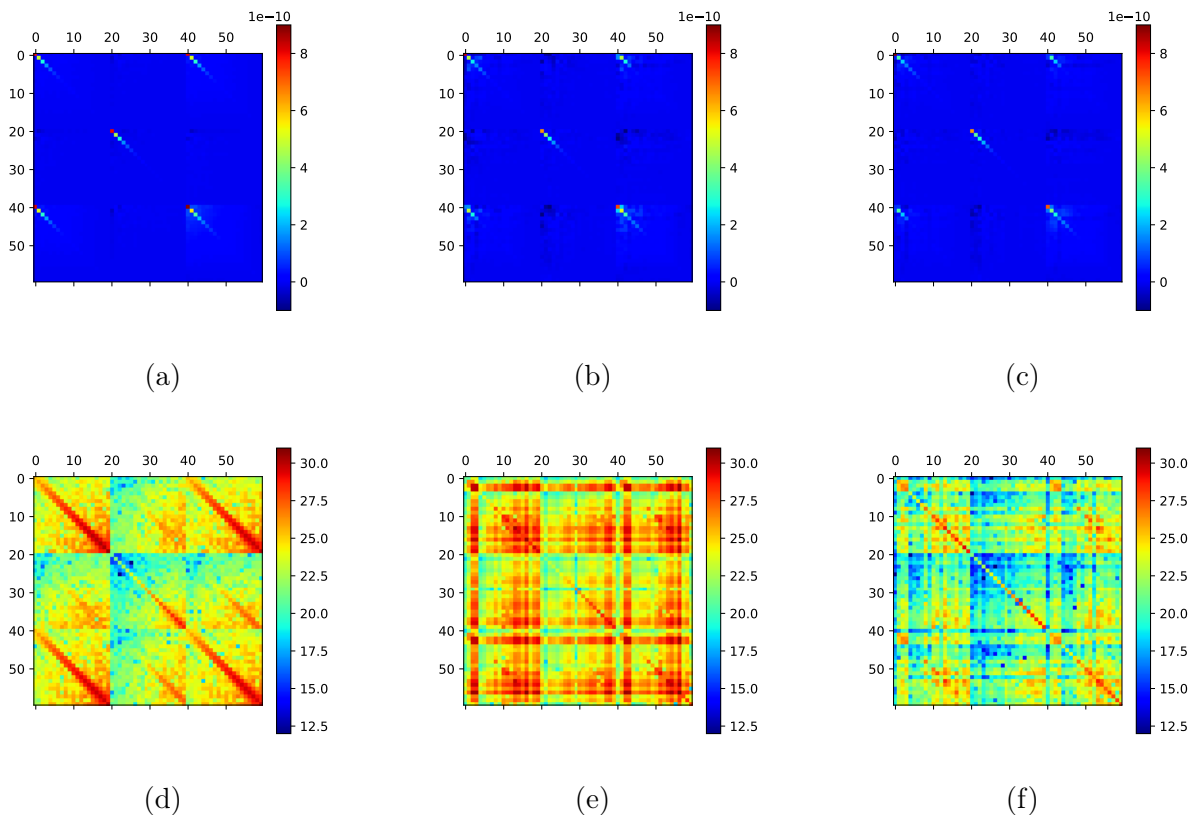


Figure 7: Covariance estimates of astronomical data of 60-dimensional data vectors. Σ is the true covariance using all 2000 data points, Σ_{MAP} is a maximum a posteriori covariance estimate using 40 data points. $\hat{\Sigma}$ is a posterior expectation estimate of Σ using 40 data points and $\hat{\Sigma}^{-1}$ is a posterior expectation estimate of Σ^{-1} using 40 data points. The posterior expectation estimate uses priors of $\sigma_1 = \sigma_2 = 2$ after normalisation and 50,000 samples from RT-RMHMC. Top left: Σ . Top middle: Σ_{MAP} . Top right: $\hat{\Sigma}$. Bottom left: $\ln |\Sigma^{-1}|$. Bottom middle: $\ln |\Sigma_{MAP}^{-1}|$. Bottom right: $\ln |\hat{\Sigma}^{-1}|$.

Metric	MAP	Posterior Expectation
$\ \Sigma - \Sigma_{EST}\ _F / \ \Sigma\ _F$	0.4862	0.5198
$\ \Sigma^{-1} - \Sigma_{EST}^{-1}\ _F / \ \Sigma^{-1}\ _F$	1.8503	0.9026
$d(\Sigma, \Sigma_{EST})$	15.2515	14.7530

Table 1

Note that in Figure 7 we have not included the sample estimate with 40 samples because the sample covariance matrix is rank deficient and hence it is not possible to invert the matrix. We notice from Figure 7 and table 1 that the MAP and Posterior Expectation perform well when estimating the covariance matrix for only using 40 data points, but lose accuracy under inversion. The posterior expectation using a sampling method seems to retain more structure when inverted and provides a more accurate estimate according to the metric of Förstner and Moonen (2003).

It is clear from Table 1 that using the posterior means do not sacrifice accuracy compared to using the MAP estimators. An additional benefit of the Bayesian approach is that we can compute posterior standard deviations for each component of the covariance estimator, which gives error estimates. This is illustrated in Figure 8. By comparing these standard deviations with the covariance estimates, we can get a sense of the relative error we are making. This information can be useful when deciding on the number of data samples we need to get a satisfactory level of accuracy in estimating the covariance matrix. Since in practice we do not have access to the true covariance matrix, there is no straightforward way to compute error estimates based on the MAP estimator, and it is challenging to see whether we have reached sufficient accuracy.

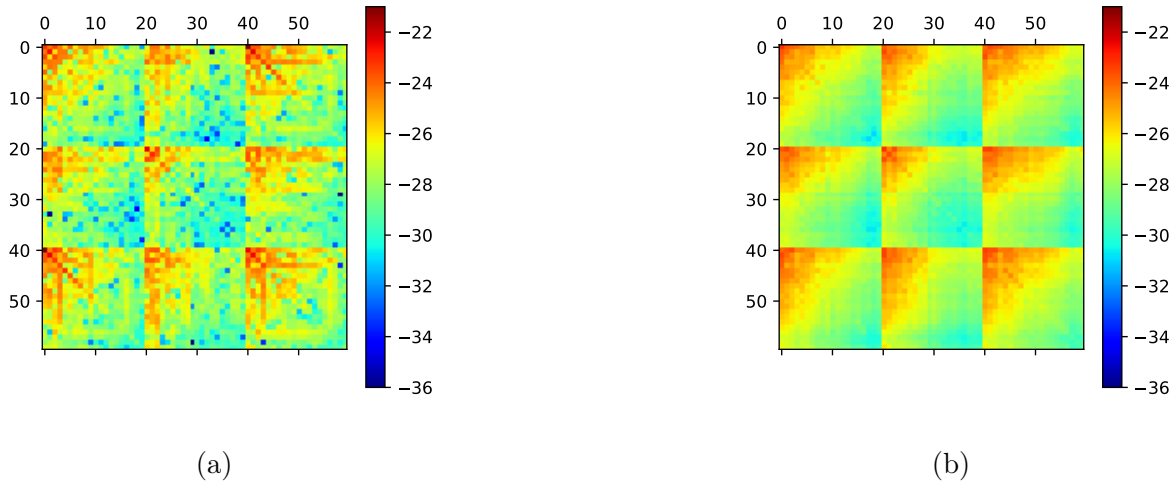


Figure 8: A comparison between the log of the absolute error and the log of the posterior standard deviations in each component. Left: $\ln|\Sigma - \hat{\Sigma}|$. Right: $\ln \Sigma_{SD}$.

7 Conclusion and Future Work

In this work we have introduced a Randomized Time Riemannian Manifold Hamiltonian Monte Carlo (RT-RMHMC), which is a robust alternative to Riemannian Manifold Hamiltonian Monte Carlo methods introduced by Girolami and Calderhead (2011) and Brubaker et al. (2012). We establish invariance of the desired measure under a compactness assumption in the continuous (small step size limit) setting. We provide an Metropolis adjusted version of RT-RMHMC in the discrete setting and prove invariance and ergodicity of the adjusted discretized algorithm. We show that RT-RMHMC is a more robust method with respect to parameter choice on a number of numerical examples arising in applications and provide an example to demonstrate that our Riemannian manifold sampling method can be used for high-dimensional covariance estimation.

In terms of future developments for RT-RMHMC, the next step would be to establish invariance of the measure in the non-compact setting and further to this establish (geometric) ergodicity of RT-RMHMC, which is already established in Bou-Rabee and Sanz-Serna (2017) for the Euclidean setting. Then one could find optimal choices of integration parameters and step-size. Another possibility would be to establish mixing time guarantees for RT-RMHMC by a coupling argument like Bou-Rabee et al. (2020) and Mangoubi and Smith (2018). In Mangoubi and Smith (2018) they establish rapid mixing guarantees for a geodesic walk algorithm on manifolds with positive curvature, which is RMHMC for the uniform distribution. One may be able to use a similar coupling argument to guarantee mixing times for RT-RMHMC for manifolds with positive curvature.

Appendices

A Additional Proofs

Lemma A.1. *Let (\mathcal{M}, g) be a smooth k -dimensional Riemannian manifold, let $K \subset \mathcal{M}$ be compact and let $R \in C^1(\mathcal{M})$ such that $R(x) > 0$ for all $x \in \mathcal{M}$, then the set*

$$\tilde{K}_R := \{(x, v) \mid x \in K, v \in T_x\mathcal{M}, |v|_g \leq R(x)\}$$

is a compact subset of $T\mathcal{M}$.

Proof. We will consider \mathcal{M} embedded in \mathbb{R}^N for $d < N$ by $i : \mathcal{M} \rightarrow \mathbb{R}^N$, then $T\mathcal{M}$ is embedded in \mathbb{R}^{2N} by an embedding $j : T\mathcal{M} \rightarrow \mathbb{R}^{2N}$. Then we will use the approach to show that $i(\tilde{K}_R)$ is closed and bounded and hence \tilde{K}_R is compact. From this point onwards all sets are embedded for ease of notation. Firstly to show that it is bounded, due to the fact that K is compact we have that

$$\|(x, v)\| \leq \|x\| + \|v\| \leq c_1 + c_2\|v\|_g \leq c_1 + c_2R(x) < \infty$$

and hence \tilde{K}_R is bounded. Now to show that it is closed we consider a convergence sequence $(x_i, v_i) \rightarrow (x, v)$ in \tilde{K}_R . We first show that $(x, v) \in TK$ by considering a local parameterisation $x \in U$, $\phi : W \rightarrow U$, where W is an open set in \mathbb{R}^k and such that we consider i sufficiently large so that (x_i, v_i) are in TU . Then $d\phi : TW \rightarrow TU$ is a diffeomorphism

which acts like $d\phi(w, z) = (\phi(w), d\phi_w(z))$ for all $(w, z) \in TW$ (see Guillemin and Pollack (1974)[Page 50]). For sufficiently large i , $(d\phi)^{-1}(x_i, v_i)$ are contained in a compact set in $TW = W \times \mathbb{R}^k$ and hence have a convergent subsequence. Then by continuity of $d\phi$ and uniqueness of limits we have that $(x, v) \in TK$. We also have that $\|v_i\|_g \leq R(x_i)$ for all i and hence by the continuity of $\|\cdot\|_g$ we have that $\|v\|_g \leq R(x)$ in the limit. Hence $v \in \tilde{K}_R$ and it is closed and hence compact. □

References

- Andersen, H. C. (1983). Rattle: A “velocity” version of the shake algorithm for molecular dynamics calculations. *Journal of Computational Physics*, 52(1):24–34.
- Barber, D. (2012). *Bayesian Reasoning and Machine Learning*. Cambridge University Press.
- Bierkens, J., Fearnhead, P., and Roberts, G. (2019). The zig-zag process and super-efficient sampling for bayesian analysis of big data. *The Annals of Statistics*, 47(3).
- Böttcher, B., Schilling, R., and Wang, J. (2013). Lévy matters. iii. *Lecture Notes in Mathematics*, 2099:71–80.
- Bou-Rabee, N., Eberle, A., and Zimmer, R. (2020). Coupling and convergence for hamiltonian monte carlo. *The Annals of applied probability*, 30(3):1209–1250.
- Bou-Rabee, N. and Sanz-Serna, J. M. (2017). Randomized hamiltonian monte carlo. *The Annals of Applied Probability*, 27(4).
- Bouchard, F., Breloy, A., Ginolhac, G., and Pascal, F. (2020). Riemannian framework for robust covariance matrix estimation in spiked models. In *ICASSP 2020-2020 IEEE International Conference on Acoustics, Speech and Signal Processing (ICASSP)*, pages 5979–5983. IEEE.
- Bouchard-Côté, A., Vollmer, S. J., and Doucet, A. (2018). The bouncy particle sampler: A nonreversible rejection-free markov chain monte carlo method. *Journal of the American Statistical Association*, 113(522):855–867.
- Brubaker, M., Salzmann, M., and Urtasun, R. (2012). A family of mcmc methods on implicitly defined manifolds. *Proceedings of the Fifteenth International Conference on Artificial Intelligence and Statistics*, PMLR, 22:161–172.
- Byrne, S. and Girolami, M. (2013). Geodesic monte carlo on embedded manifolds. *Scandinavian Journal of Statistics*, 40(4):825–845.
- Cai, T., Ma, Z., and Wu, Y. (2015). Optimal estimation and rank detection for sparse spiked covariance matrices. *Probability theory and related fields*, 161(3):781–815.
- Casella, C. R. G. (2004). *Monte Carlo Statistical Methods*. Springer Texts in Statistics. Springer, 2nd edition.

- Chamberlain, G. and Rothschild, M. (1982). Arbitrage, factor structure, and mean-variance analysis on large asset markets.
- Chicone, C. (2006). *Ordinary Differential Equations with Applications*. Texts in Applied Mathematics. Springer New York.
- Davis, M. H. A. (1993). *Markov Models & Optimization*.
- Deligiannidis, G., Paulin, D., Bouchard-Côté, A., and Doucet, A. (2021). Randomized Hamiltonian Monte Carlo as scaling limit of the bouncy particle sampler and dimension-free convergence rates. *The Annals of Applied Probability*, 31(6):2612 – 2662.
- Diaconis, P., Holmes, S., and Shahshahani, M. (2013). Sampling from a manifold. In *Advances in modern statistical theory and applications: a Festschrift in honor of Morris L. Eaton*, pages 102–125. Institute of Mathematical Statistics.
- Durmus, A., Guillin, A., and Monmarché, P. (2021). Piecewise deterministic markov processes and their invariant measures. In *Annales de l’Institut Henri Poincaré, Probabilités et Statistiques*, volume 57, pages 1442–1475. Institut Henri Poincaré.
- Ethier, S. N. and Kurtz, T. G. (1986). *Markov processes. Characterization and convergence*. John Wiley & Sons Inc.
- Fan, J., Fan, Y., and Lv, J. (2008). High dimensional covariance matrix estimation using a factor model. *Journal of Econometrics*, 147(1):186–197.
- Förstner, W. and Moonen, B. (2003). A metric for covariance matrices. In *Geodesy—the Challenge of the 3rd Millennium*, pages 299–309. Springer.
- Girolami, M. and Calderhead, B. (2011). Riemann manifold langevin and hamiltonian monte carlo methods. *Journal of the Royal Statistical Society: Series B (Statistical Methodology)*, 73(2):123–214.
- Graham, M. M., Thiery, A. H., and Beskos, A. (2021). Manifold markov chain monte carlo methods for bayesian inference in a wide class of diffusion models. *arXiv preprint arXiv:1912.02982*.
- Greenberg, E. (2012). *Introduction to Bayesian Econometrics*. Cambridge University Press, 2 edition.
- Guillemin, V. and Pollack, A. (1974). *Differential Topology*. AMS Chelsea Publishing.
- Hairer, E., Hochbruck, M., Iserles, A., and Lubich, C. (2006). Geometric numerical integration. *Oberwolfach Reports*, 3(1):805–882.
- Hamelryck, T., Kent, J. T., and Krogh, A. (2006). Sampling realistic protein conformations using local structural bias. *PLOS Computational Biology*, 2(9):1–13.
- Hartmann, C. (2007). Model reduction in classical molecular dynamics.
- Hartmann, C. (2008). An ergodic sampling scheme for constrained hamiltonian systems with applications to molecular dynamics. *Journal of Statistical Physics*, 130(4):687–711.

- Hoffman, M. D., Gelman, A., et al. (2014). The no-u-turn sampler: adaptively setting path lengths in hamiltonian monte carlo. *J. Mach. Learn. Res.*, 15(1):1593–1623.
- Joachimi, B. (2017). Non-linear shrinkage estimation of large-scale structure covariance. *Monthly Notices of the Royal Astronomical Society: Letters*, 466(1):L83–L87.
- Jolliffe, I. (1986). Generalizations and adaptations of principal component analysis. In *Principal Component Analysis*, pages 223–234. Springer.
- Kleppe, T. S. (2022). Connecting the dots: Numerical randomized hamiltonian monte carlo with state-dependent event rates. *Journal of Computational and Graphical Statistics*, (just-accepted):1–41.
- Kritchman, S. and Nadler, B. (2008). Determining the number of components in a factor model from limited noisy data. *Chemometrics and Intelligent Laboratory Systems*, 94(1):19–32.
- Kunze, K. and Schaeben, H. (2004). The bingham distribution of quaternions and its spherical radon transform in texture analysis. *Mathematical Geology*, 36(8):917 – 943.
- Lam, C. (2016). Nonparametric eigenvalue-regularized precision or covariance matrix estimator. *The Annals of Statistics*, 44(3):928–953.
- Lam, C. (2020). High-dimensional covariance matrix estimation. *WIREs Computational Statistics*, 12(2):e1485.
- Laurent, A. and Vilmart, G. (2021). Order conditions for sampling the invariant measure of ergodic stochastic differential equations on manifolds. *Foundations of Computational Mathematics*, pages 1–47.
- Lee, T., Leok, M., and McClamroch, N. H. (2017). Global formulations of lagrangian and hamiltonian dynamics on manifolds. *Springer*, 13:31.
- Leimkuhler, B. and Matthews, C. (2016). Efficient molecular dynamics using geodesic integration and solvent-solute splitting. *Proceedings of the Royal Society A: Mathematical, Physical and Engineering Sciences*, 472(2189):20160138.
- Leimkuhler, B. and Reich, S. (2004). *Simulating Hamiltonian Dynamics*. Cambridge: Cambridge University Press.
- Leimkuhler, B. J. and Skeel, R. D. (1994). Symplectic numerical integrators in constrained hamiltonian systems. *Journal of Computational Physics*, 112(1):117–125.
- Lelièvre, T., Rousset, M., and Stoltz, G. (2010). *Free Energy Computations*. Imperial College Press.
- Lelièvre, T., Rousset, M., and Stoltz, G. (2012). Langevin dynamics with constraints and computation of free energy differences. *Mathematics of computation*, 81(280):2071–2125.
- Lelièvre, T., Rousset, M., and Stoltz, G. (2019). Hybrid monte carlo methods for sampling probability measures on submanifolds. *Numerische Mathematik*, 143(2):379–421.

- Mangoubi, O. and Smith, A. (2018). Rapid mixing of geodesic walks on manifolds with positive curvature. *The Annals of Applied Probability*, 28(4):2501–2543.
- Mardia, K. V., Jupp, P. E., and Mardia, K. (2000). *Directional statistics*, volume 2. Wiley Online Library.
- Marsden, J. E. and West, M. (2001). Discrete mechanics and variational integrators. *Acta Numerica*, 10:357–514.
- Meyer, G., Bonnabel, S., and Sepulchre, R. (2011). Linear regression under fixed-rank constraints: A riemannian approach. In *Proceedings of the 28th International Conference on International Conference on Machine Learning*, ICML’11, page 545–552, Madison, WI, USA. Omnipress.
- Nash, J. (1956). The imbedding problem for riemannian manifolds. *Annals of mathematics*, pages 20–63.
- Ortega, J. M. and Rheinboldt, W. C. (2000). *Iterative solution of nonlinear equations in several variables*. SIAM.
- Pakman, A., Gilboa, D., Carlson, D., and Paninski, L. (2017). Stochastic bouncy particle sampler. In Precup, D. and Teh, Y. W., editors, *Proceedings of the 34th International Conference on Machine Learning*, volume 70 of *Proceedings of Machine Learning Research*, pages 2741–2750. PMLR.
- Perez, A., MacCallum, J. L., and Dill, K. A. (2015). Accelerating molecular simulations of proteins using bayesian inference on weak information. *Proceedings of the National Academy of Sciences*, 112(38):11846–11851.
- Quiroz, M., Kohn, R., Villani, M., and Tran, M.-N. (2018). Speeding up mcmc by efficient data subsampling. *Journal of the American Statistical Association*.
- Riou-Durand, L. and Vogrin, J. (2022). Metropolis adjusted langevin trajectories: a robust alternative to hamiltonian monte carlo. *arXiv preprint arXiv:2202.13230*.
- Ross, S. A. (2013). The arbitrage theory of capital asset pricing. In *Handbook of the fundamentals of financial decision making: Part I*, pages 11–30. World Scientific.
- Salakhutdinov, R. and Mnih, A. (2008). Bayesian probabilistic matrix factorization using markov chain monte carlo. In *ICML ’08*.
- Shen, D., Shen, H., and Marron, J. (2016). A general framework for consistency of principal component analysis. *The Journal of Machine Learning Research*, 17(1):5218–5251.
- Tierney, L. (1994). Markov Chains for Exploring Posterior Distributions. *The Annals of Statistics*, 22(4):1701 – 1728.
- Vanetti, P., Bouchard-Côté, A., Deligiannidis, G., and Doucet, A. (2018). Piecewise-deterministic markov chain monte carlo. *arXiv preprint arXiv:1707.05296*.

- Wilkinson, D. J. (2007). Bayesian methods in bioinformatics and computational systems biology. *Briefings in Bioinformatics*, 8(2):109–116.
- Zappa, E., Holmes-Cerfon, M., and Goodman, J. (2018). Monte carlo on manifolds: Sampling densities and integrating functions. *Communications on Pure and Applied Mathematics*, 71(12):2609–2647.